TM-70-2011-3

TECHNICAL MEMORANDUM

VIRTUAL MASS TECHNIQUE FOR COMPUTING N-BODY SOLUTIONS

Bellcomm

BELLCOMM, INC.
955 L'ENFANT PLAZA NORTH, S.W., WASHINGTON, D.C. 20024

COVER SHEET FOR TECHNICAL MEMORANDUM

TITLE- Virtual Mass Technique for Computing N-Body Solutions

TM-70-2011-3

DATE- December 28, 1970

FILING CASE NO(S)- 103-9

AUTHOR(S)- D. H. Novak

FILING SUBJECT(S) (ASSIGNED BY AUTHOR(S))- Trajectory Analysis
Celestial Mechanics
Interplanetary Trajectories
Lunar Trajectories

ABSTRACT

A new N-body numerical integration procedure has been developed using the Virtual Mass concept. A fictitious Virtual Mass force center is defined in terms of its magnitude and relative location so as to produce the same instantaneous gravitational acceleration of a body in space as is produced by the totality of the real celestial bodies acting upon it. This concept is a generalization of the gravispheric force center of the three-body problem to the case of an arbitrary number of gravitating bodies. The self-starting integration method is Encke-like in that, over each computing interval, a reference conic is computed relative to a constant magnitude Virtual Mass. However, the auxiliary acceleration equation is solved for not just the reference-conic-to-true trajectory perturbation, but rather for this quantity plus the Virtual Mass inertial motion. The method of solution is an iterative procedure for determining the coefficients of a Taylor's series expansion of the combined correction term so that the acceleration and jerk are satisfied at specified points on the computing interval. Coefficients through the fifth order can be determined by matching the acceleration and jerk at the computing interval end points only. Double precision digital computer comparisons have shown this fifth order expansion to be very efficient, yet highly accurate with large interval sizes.

SEE REVERSE SIDE FOR DISTRIBUTION LIST

DISTRIBUTION LIST (CONT.)

Marshall Space Flight Center (Cont.)

H. G. Krause/S&E-AERO-T
J. Lindberg/S&E-AERO-M
H. J. Sperling/S&E-AERO-T
H. F. Thomae/PD-DO-P
G. Wittenstein/S&E-AERO-MFT
A. C. Young/PD-DO-S

Analytical Mechanics Associates

J. B. Eades
J. T. Findlay
M. G. Kelly
S. Pines
H. Wolf

The Boeing Company

J. Coons
A. Deprit

Martin-Marietta Corporation

W. J. Pragluski

McDonnell-Douglas Astronautics Co.

J. E. Lancaster

MIT - Instrumentation Laboratory

R. H. Battin
T. N. Edelbaum
D. C. Fraser

Purdue University

D. W. Alspaugh
H. Lo
H. Pollard

Smithsonian Astrophysical Observatory

C. A. Lundquist
B. G. Marsden

DISTRIBUTION LIST (CONT.)

The University of Texas at Austin

D. G. Hull
P. E. Nacozy
V. Szebehely
B. D. Tapley

U. S. Naval Observatory

R. L. Duncombe
A. D. Fiala
W. Klepczynski
P. K. Seidelmann
T. C. Van Flandern

Bellcomm, Inc.

G. M. Anderson
R. A. Bass
H. B. Bosch
A. P. Boysen, Jr.
M. V. Bullock
J. O. Cappellari, Jr.
K. M. Carlson
D. A. Corey
D. A. De Graaf
A. J. Ferrari
L. P. Gieseler
E. M. Grenning
D. R. Hagner
W. G. Heffron
N. W. Hinners
T. B. Hoekstra
R. F. Jessup
S. L. Levie, Jr.
D. P. Ling
H. S. London
D. Macchia
K. E. Martersteck
W. I. McLaughlin
J. Z. Menard
G. T. Orrok
R. J. Stern
C. C. H. Tang
J. W. Timko
R. L. Wagner
G. D. Wolske
T. L. Yang
Department 1024 File

DISTRIBUTION LIST (CONT.)

COVER SHEET ONLY TO

K. R. Carpenter
J. P. Downs
F. El-Baz
A. N. Kontaratos
M. Liwshitz
J. L. Marshall, Jr.
P. E. Reynolds
P. S. Schaenman
F. N. Schmidt
A. R. Vernon
M. P. Wilson

TABLE OF CONTENTS

LIST OF FIGURES

BELLCOMM, INC.
955 L'ENFANT PLAZA NORTH, S.W. WASHINGTON, D. C. 20024

SUBJECT: Virtual Mass Technique for Computing N-Body Solutions

DATE: December 28, 1970

FROM: D. H. Novak

TM-70-2011-3

TECHNICAL MEMORANDUM

1.0 INTRODUCTION

This memorandum is concerned with the problem of computing a spacecraft trajectory with high precision, given initial conditions of position and velocity at a specified time. Initially, the spacecraft is assumed to be acted upon only by inverse square gravitational forces of attraction exerted by n mathematical point masses representing n large celestial bodies such as the Sun, planets, and possibly their moons. The treatment will be modified later to include non-gravitational forces (e.g., rocket thrust and solar radiation pressure) and the asphericity of the potentials of the individual celestial bodies.

The celestial bodies themselves are acted upon by their mutual gravitational attractions; hence, the complete set of differential equations of motion for the entire system of bodies (n gravitating bodies plus the spacecraft) is

$$\left.\begin{aligned} \ddot{\bar{r}}_s &= -\sum_{i=1}^{n} \frac{\mu_i \bar{r}_{is}}{r_{is}^3} \\ \ddot{\bar{r}}_j &= -\sum_{i=1}^{n} \frac{\mu_i \bar{r}_{ij}}{r_{ij}^3} \qquad (j=1,\ldots,n) \qquad (i\neq j) \end{aligned}\right\} \quad (1)$$

In these equations

μ_i = mass of the $i^{\underline{th}}$ body times the Universal Gravitation Constant G

$\bar{r}_i$ = inertial position of the $i^{\underline{th}}$ body

$\bar{r}_s$ = inertial position of the spacecraft

$$\bar{r}_{is} = \bar{r}_s - \bar{r}_i$$

$$r_{is} = |\bar{r}_{is}|$$

Equations (1) and the appropriate initial conditions mathematically define the classical restricted N-body (N = n+1) problem. Clearly, all n large bodies influence the inertial motion of the spacecraft in Eqn. (1a), whereas none of these large bodies is influenced in Eqn. (1b) by the spacecraft. Thus, the system of Eqns. (1b) is uncoupled from Eqn. (1a) and can be solved separately once and for all to give the ephemeris of the system of celestial bodies in the form of time-histories of $\bar{r}_i$. These data can be used in Eqn. (1a) to solve for the remaining unknown, $\bar{r}_s(t)$, subject to specified initial conditions.

It is well known that the general solution to the system of Eqns. (1) for n = 1 is the conic section given by the intersection of the three-dimensional surface

$$\bar{e}\cdot\bar{r}_s + r_s = \frac{H^2}{\mu} \tag{2}$$

with the plane through the origin ($\bar{r}_s = 0$) orthogonal to $\bar{H}$. The constant vectors $\bar{e}$ and $\bar{H}$ define the orbital elements, and are given by the initial conditions:

$$\left.\begin{aligned} \bar{H} &= \bar{r}_{s_o} \times \dot{\bar{r}}_{s_o} \\ \bar{e} &= -\frac{\bar{r}_{s_o}}{r_{s_o}} - \frac{\bar{H} \times \dot{\bar{r}}_{s_o}}{\mu} \end{aligned}\right\} \tag{3}$$

In writing Eqns. (2) and (3), it has been tacitly assumed that the inertial origin is taken at the center of the solitary

gravitating body. The development and use of the two-body solution in this three-dimensional vector form is treated in detail in Reference 7. This computationally convenient form is used in the procedure described here.

Just as well known as this two body solution is the fact that the general solution to Eqns. (1) has not been found for n > 1. Therefore, it is necessary to resort to numerical techniques to obtain solutions to Eqns. (1) or (1a) for the many-body case. For the sake of clarity in presentation of subsequent concepts, two categories of numerical solutions will be considered:

(1) Exact (analytical) solution of approximate differential equations of motion over the computing interval.

(2) Approximate solution of exact differential equations of motion over the computing interval.

Since the only known general analytical solution is the two body conic solution given by Eqns. (2) and (3), the first category involves reduction of Eqn. (1a) to a single gravitating body. Historically, this has been accomplished quite simply by neglecting all but the single dominant term on the right-hand side. As long as the same term (hence the same celestial body) dominates the contributions of the others, there is no point in breaking up the solution into short arcs. The exact solution should be propagated in one step over the entire range of applicability. Thus, the classical "patched conic" procedure represents the spacecraft trajectory as a series of conic arcs, spanning the corresponding spheres of influence and patched together at the boundaries such that the appropriately transformed trajectory states agree. As an illustrative example, a simple one-way interplanetary trajectory to Mars would be computed as three conic arcs: (1) a geocentric portion within the Earth's sphere of influence (SOI), (2) a heliocentric arc from the Earth's SOI to Mars' SOI and (3) a Mars-centered section within its SOI. Such trajectories can be computed quite rapidly. However, as might be expected from the oversimplification involved in the assumptions, the accuracy is low. The answers are good enough for gross mission planning purposes, but not for detailed design and execution.

The second category (approximate solutions to exact equations) provides a means for computing highly accurate trajectories. The fundamental principle rests upon assuming

some functional form for the solution over a small computation interval. The free parameters of the function are then adjusted so as to best satisfy (in some sense) the differential equation and the spacecraft state at the beginning of the interval. The details differ from one integration scheme to the next. As an example, the functional form could be assumed as a truncated power series in the independent time variable. The coefficients could then be solved for in order to satisfy the interval initial conditions and the differential equation at selected sub-interval time points. As far as astrodynamic applications are concerned, there are two further subclassifications of this second category into the Cowell and Encke methods.

The Cowell method represents the entire solution with the approximating functional form, treating all terms on the right-hand side of Eqn. (1a) as contributors of equal weight. Thus, it is necessary to carry a large number of significant digits in the computations so as not to lose the contributions of the small perturbations, taken together with the dominant term(s). In addition, it is necessary to compute with relatively small step sizes in order to keep the errors in the approximating function small. Clearly, one does not realize a smaller and smaller error as the step size is decreased, due to the precision limitation inherent in finite digit truncation. The optimal interval size can be determined for each scheme by numerical experiments.

The Encke method separates the complete solution into a reference trajectory and a perturbative correction. Let us denote the dominant celestial body by n = 1. Then write the inertial spacecraft position as

$$\bar{r}_s = \bar{r}_{1s} + \bar{r}_1 \tag{4}$$

Now introduce the reference trajectory with respect to the dominant body n = 1:

$$\bar{r}_{1s} = \bar{r}_{1r} + \bar{r}_{rs} \tag{5}$$

where $\bar{r}_{1r}$ satisfies the two-body differential equation:

$$\ddot{\bar{r}}_{1r} = - \frac{\mu_1 \bar{r}_{1r}}{r_{1r}^3} \tag{6}$$

with initial conditions at some epoch t_E:

$$\left.\begin{aligned} \bar{r}_{1r}\ (t_E) &= \bar{r}_{1s}\ (t_E) \\ \dot{\bar{r}}_{1r}\ (t_E) &= \dot{\bar{r}}_{1s}\ (t_E) \end{aligned}\right\} \tag{7}$$

Thus, the reference conic is said to "osculate" the true orbit at the epoch t_E and, by Eqns. (5) and (7), we see that

$$\bar{r}_{rs}\ (t_E) = \dot{\bar{r}}_{rs}\ (t_E) = 0 \tag{8}$$

Substituting Eqn. (5) into Eqn. (4), differentiating twice and substituting from Eqns. (1) and (6) leads finally to the perturbation differential equation:

$$\ddot{\bar{r}}_{rs} = \frac{\mu_1 \bar{r}_{1r}}{r_{1r}^3} - \frac{\mu_1 \bar{r}_{1s}}{r_{1s}^3} + \sum_{i=2}^{n} \mu_i \left(\frac{\bar{r}_{il}}{r_{il}^3} - \frac{\bar{r}_{is}}{r_{is}^3} \right) \tag{9}$$

This is the equation that is solved, subject to initial conditions (8), by means of the approximating function. As written in Eqn. (9), there are obvious computational difficulties associated with small differences of nearly equal quantities. These difficulties can be circumvented by appropriate algebraic manipulation of the right-hand side to obtain equivalent expressions in terms of the perturbation quantity $\bar{r}_{rs}$. (See Ref. 1, for example).

The advantage of the Encke procedure lies in the fact that, where the spacecraft motion is dominated by one celestial body, the perturbation is small, and hence the effect of errors of the approximating function are minimized. Generally, the perturbation solution can be computed to fewer significant digits than must be carried in the Cowell method. When the perturbation grows too large, a "rectification" can be made to establish a new reference conic, starting at the new epoch. The rectification, of course, reduces the perturbation solution to the zero values (Eqn. (8)).

The numerical procedure developed here is based on a new concept, the Virtual Mass technique, originally reported in Ref. 3. The concept of the gravispheric force center for the restricted problem of three bodies was published in Ref. 2, but is not widely known. Although the gravisphere itself cannot be generalized to $n > 2$ bodies, it is shown in Ref. 3 that the equations for the force center and its associated mass magnitude can be generalized for such cases. At any instant, the unique fictitious body defined by this force center and mass magnitude produces precisely the same inertial acceleration of the spacecraft as that produced by the actual celestial bodies.

The existence of this "Virtual Mass" immediately suggests the possibility of a simple implementation of a first category computational procedure -- an exact solution of an approximation to the equations of motion over each computing interval. Specifically, the spacecraft motion could be represented as a conic arc over each computing interval, relative to an unaccelerated Virtual Mass of constant magnitude. Several such schemes were programmed for the computer and studied in Ref. 3. The best mechanization yielded an accuracy of 2 parts in 7×10^6 for the Jacobi energy for a restricted three-body circumlunar trajectory.

This accuracy is adequate for the computation of design and operational lunar trajectories, since it exceeds the requirements for estimation and control of such trajectories. The requirements for interplanetary trajectories, on the other hand, are orders of magnitude greater due to their far greater sensitivities. Accordingly, the specific purpose of this memorandum is to document a new Virtual Mass computational procedure of the second category. The spacecraft motion is separated into a reference trajectory and a perturbative correction à la Encke.

The reference trajectory is an osculating conic section relative to the Virtual Mass. However, since the Virtual Mass motion is not known a priori, as is the physically real reference body in the usual Encke procedure, the perturbative correction and the Virtual Mass motion are lumped together and expanded in a single Taylor's series. The evaluation of the coefficients of this series includes the effects of the Virtual Mass magnitude change as well as the position change. It will be seen that this more sophisticated procedure is still quite concise and hence fast.

For the sake of completeness, and since Ref. 3 saw only limited distribution, the derivation of the basic Virtual Mass equations is included, together with the equations for the new computational procedure.

2.0 THE VIRTUAL MASS CONCEPT

As stated in the Introduction, the main interest in this memorandum is the motion of a spacecraft in the restricted N-body problem. However, it should be borne in mind that the concept of the Virtual Mass is in no way dependent upon the fact that the spacecraft mass is infinitesimal compared with that of the celestial bodies. Each celestial body also has an associated Virtual Mass which can be used, in an obvious extension of the procedure to be described for the spacecraft alone, to solve the general N-body problem.

The Virtual Mass principle (for a spacecraft) is based upon the idea of replacing the combined gravitational effects of many celestial bodies on the spacecraft by the attraction of a single equivalent body.* The line of action of the resultant gravitational force vector defines the locus of possible force center locations (the mass magnitude is uniquely related to the location). The force center location, called the 'varicenter', chosen in Ref. 4 not only gave the correct force but also matched the instantaneous gradient of that force. However, in order to use this force center in a practical integration scheme, it was necessary to take into account the dynamics of the varicenter motion. The significance of this will become more apparent in the subsequent presentation of different methods of utilizing the Virtual Mass.

---

*This is not a new idea. For example, an attempt was made in Ref. 4 to make an instantaneous reduction of the restricted N-body problem for implementation as an integration method, while Ref. 5 describes a procedure for replacing the Earth and Moon by a single body to permit accurate navigation and guidance on lunar missions using the two-body equations.

As noted earlier, the Virtual Mass location and magnitude are derived as the n-body generalization of the gravispheric force center. Because of the relative obscurity of the concept of the gravispheric force center, the development will begin with a presentation of this material. More importantly, this affords an opportunity to express the results in particular algebraic forms which reduce to a triviality the subsequent generalization to more than two gravitating bodies.

2.1 The Gravisphere

Consider the simple system consisting of two large magnitude point masses μ_1 and μ_2 and a spacecraft S. As mentioned earlier, the mass of the third body need not be infinitesimal compared with μ_1 and μ_2. The symbol μ, used here to designate the mass points, quantitatively represents the mass times the Universal Gravitation Constant. The position vectors of the three bodies are denoted by $\bar{r}_1$, $\bar{r}_2$, and $\bar{r}_s$ in an arbitrary inertial reference frame (Fig. 1). The relative positions are

$$\left.\begin{aligned} \bar{r}_{1s} &= \bar{r}_s - \bar{r}_1 \\ \bar{r}_{2s} &= \bar{r}_s - \bar{r}_2 \\ \bar{r}_{12} &= \bar{r}_2 - \bar{r}_1 \end{aligned}\right\} \tag{10}$$

We will now determine the nature of the surface defining the locus of all possible spacecraft positions having the constant ratio

$$\rho \triangleq \frac{r_{1s}}{r_{2s}} \tag{11}$$

where, of course,

$$\rho = \frac{r_{1S}}{r_{2S}} = \text{CONST.}$$

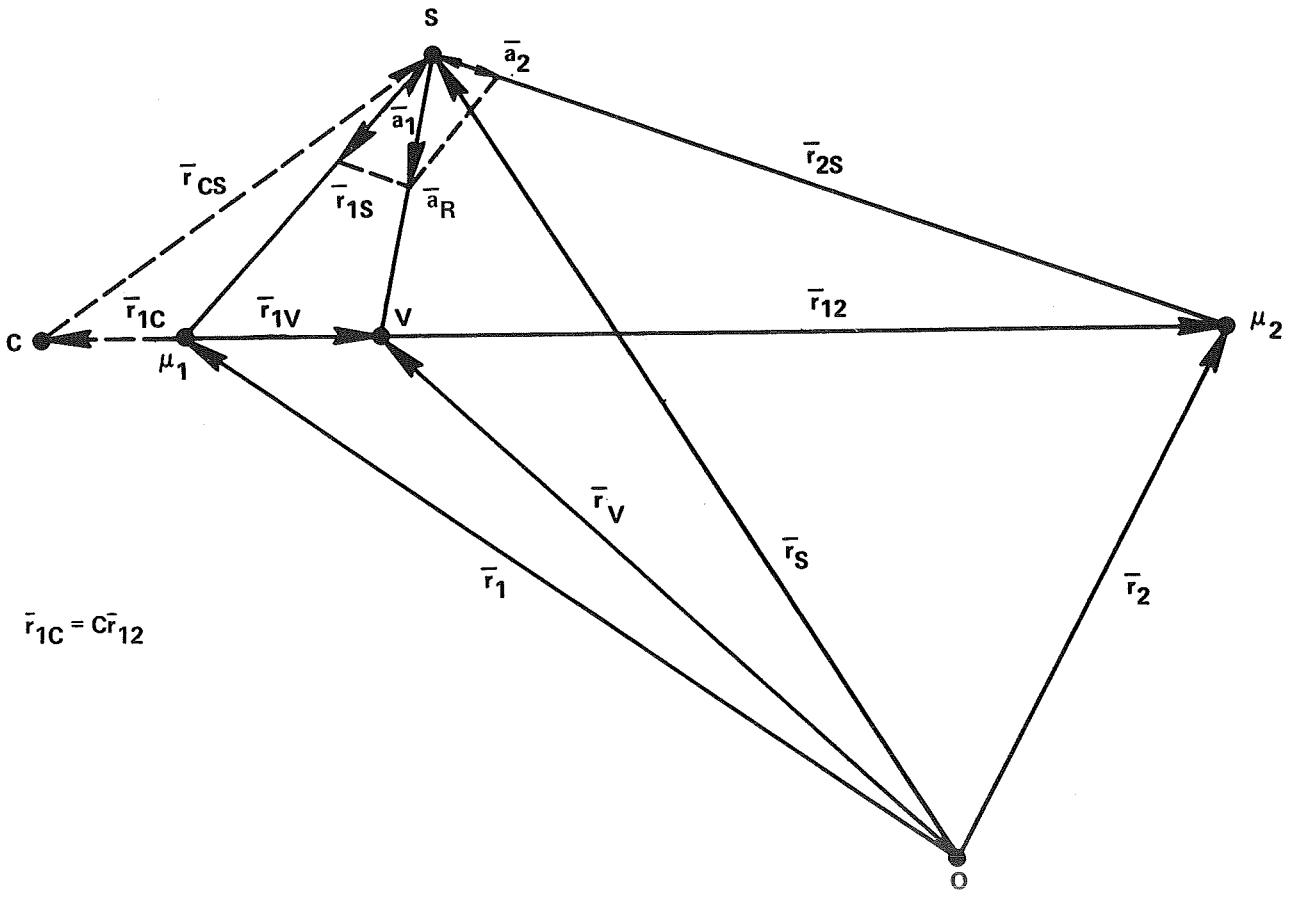

$\bar{r}_{1C} = C\bar{r}_{12}$

FIGURE 1 - GEOMETRY OF GRAVISPHERIC FORCE CENTER

$$r_{1s} \triangleq |\bar{r}_{1s}|$$

$$r_{2s} \triangleq |\bar{r}_{2s}|$$

It is anticipated that this surface must be rotationally symmetric about the line $\bar{r}_{12}$. Clearly, then, it will be more convenient to express the spacecraft position in terms of a coordinate system centered on this axis. Let C be a scalar factor to be applied to $\bar{r}_{12}$, defining the fractional displacement of this new coordinate frame origin from mass point μ_1 toward μ_2 (see Fig. 1). The value of C will be left arbitrary for the moment, but will be evaluated later to afford the greatest convenience in interpreting the analytical form for the surface. Now write

$$\bar{r}_s = \bar{r}_1 + C\bar{r}_{12} + \bar{r}_{cs}$$

and substitute this into Eqn. (10) to obtain

$$\left.\begin{aligned} \bar{r}_{1s} &= \bar{r}_{cs} + C\bar{r}_{12} \\ \bar{r}_{2s} &= \bar{r}_{cs} + C\bar{r}_{12} + \bar{r}_1 - \bar{r}_2 = \bar{r}_{cs} + (C-1)\bar{r}_{12} \end{aligned}\right\} \quad (12)$$

The magnitudes of these vectors are

$$\left.\begin{aligned} r_{1s}^2 &= \bar{r}_{1s}\cdot\bar{r}_{1s} = r_{cs}^2 + C^2 r_{12}^2 + 2C\bar{r}_{12}\cdot\bar{r}_{cs} \\ r_{2s}^2 &= \bar{r}_{2s}\cdot\bar{r}_{2s} = r_{cs}^2 + (C-1)^2 r_{12}^2 + 2(C-1)\bar{r}_{12}\cdot\bar{r}_{cs} \end{aligned}\right\} \quad (13)$$

Squaring Eqn. (11) and substituting from Eqns. (13) yields

$$r_{cs}^2 + C^2 r_{12}^2 + 2C\bar{r}_{12}\cdot\bar{r}_{cs} = \rho^2[r_{cs}^2 + (C-1)^2 r_{12}^2 + 2(C-1)\bar{r}_{12}\cdot\bar{r}_{cs}]$$

Collecting like terms and dividing through by $1-\rho^2$:

$$r_{cs}^2 + 2\bar{r}_{cs}\cdot\bar{r}_{12}\left(C + \frac{\rho^2}{1-\rho^2}\right) + r_{12}^2\left[C^2 + \frac{(2C-1)\rho^2}{1-\rho^2}\right] = 0 \qquad (14)$$

The most convenient choice for C is clearly

$$C = -\frac{\rho^2}{1-\rho^2} \qquad (15)$$

since this causes the second term in Eqn. (14) to vanish. Substituting Eqn. (15) into Eqn. (14) shows finally that the surface is a sphere with center at $C\bar{r}_{12}$ relative to μ_1 and with radius

$$r_{cs} = \left|\frac{\rho}{1-\rho^2}\right| r_{12} \qquad (16)$$

Since the ratio of the distances from the two large masses is constant on this sphere, and since the gravitational attraction depends inversely upon distance squared, the ratio of the two gravitational attractions is also constant -- hence the name gravisphere. The geometry of the family of gravispheres is shown in Fig. 2 for several different values of ρ. Observe that when the spacecraft position corresponds with μ_1, then $r_{1s} = 0$, $\rho = 0$, the geometric center of the gravisphere is also at the point μ_1, and by Eqn. (16) the radius $r_{cs} = 0$. As the spacecraft moves away from μ_1, the geometric center also moves away in a negative direction (away from μ_2) along $\bar{r}_{12}$. When

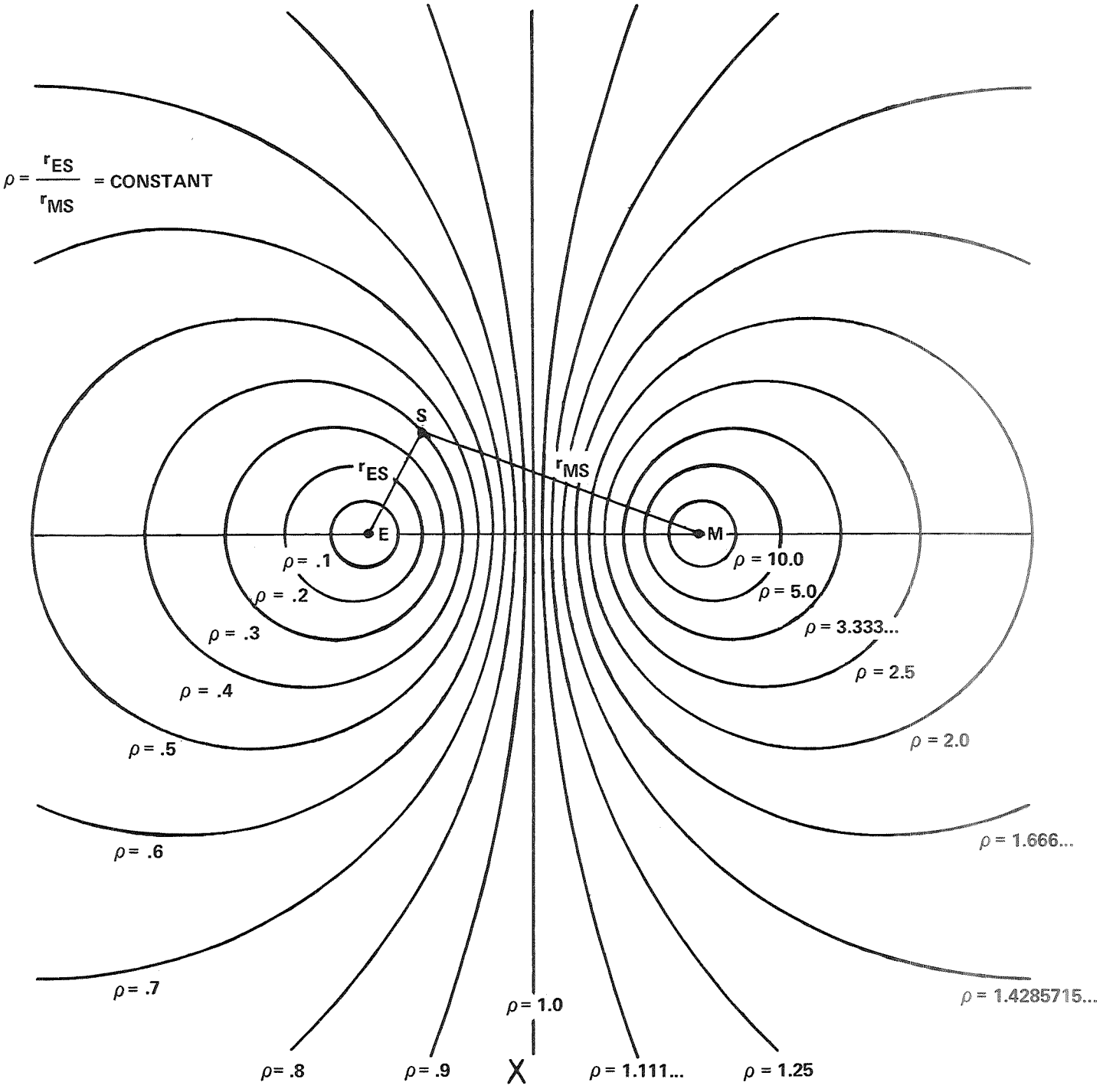

FIGURE 2 - GEOMETRY OF GRAVISPHERES

the spacecraft is equidistant from both bodies, $\rho = 1$, the gravisphere radius is infinite, and the geometric center is at $\pm \infty$ along $\bar{r}_{12}$. In this case, of course, the gravisphere is actually the plane equally dividing all space between the two masses. Finally, as the spacecraft moves toward μ_2, ρ increases from 1 to $+\infty$, and the gravisphere collapses on μ_2 as the geometric center moves from $+\infty$ (away from μ_1) to μ_2 on $\bar{r}_{12}$. Note that, since this geometry is completely independent of the mass values μ_1 and μ_2, there is not only rotational symmetry about $\bar{r}_{12}$ but also a mirror symmetry with respect to the halfway plane $\rho = 1$. The influence of the mass magnitudes will be considered in the next section.

2.2 The Gravispheric Force Center

To facilitate the identification of arbitrary points on the surface of a gravisphere, let us introduce an arbitrarily oriented unit vector $\bar{n}$. Using this vector, together with the radius magnitude given by Eqn. (16), the vector from the geometric center of a gravisphere (defined by a value of ρ) to any spacecraft position on that gravisphere can be written as

$$\bar{r}_{cs} = \frac{\rho}{1-\rho^2} r_{12} \bar{n} \tag{17}$$

The absolute value symbol is omitted from the factor involving ρ, since the sign is assumed to be absorbed in $\bar{n}$ itself. For the sake of algebraic convenience, let us also introduce $\bar{u}$, a unit vector in the direction of $\bar{r}_{12}$. Therefore, one may write

$$\bar{r}_{12} = r_{12} \bar{u} \tag{18}$$

Now, substitute Eqns. (15), (17) and (18) into Eqn. (12) to obtain

$$\left.\begin{aligned} \bar{r}_{1s} &= \frac{\rho r_{12}}{1-\rho^2}\,(\bar{n} - \rho\bar{u}) \\ \bar{r}_{2s} &= \frac{r_{12}}{1-\rho^2}\,(\rho\bar{n} - \bar{u}) \end{aligned}\right\} \tag{19}$$

According to the inverse square law of gravitational attraction, the acceleration of the spacecraft is written as

$$\bar{A}_R = -\frac{\mu_1\bar{r}_{1s}}{r_{1s}^3} - \frac{\mu_2\bar{r}_{2s}}{r_{2s}^3}$$

From Eqn. (11)

$$r_{1s} = \rho r_{2s}$$

Hence, the resultant acceleration can be written in the form

$$\bar{A}_R = -\frac{1}{r_{2s}^3}\left(\frac{\mu_1\bar{r}_{1s}}{\rho^3} + \mu_2\bar{r}_{2s}\right)$$

Substituting Eqn. (19) into this expression and collecting like terms gives

$$\bar{A}_R = -\frac{r_{12}}{(1-\rho^2)r_{2s}^3}\left[\left(\frac{\mu_1}{\rho^2} + \mu_2\rho\right)\bar{n} - \left(\frac{\mu_1}{\rho} + \mu_2\right)\bar{u}\right] \tag{20}$$

Recognizing that $\bar{A}_R$ always intersects $\bar{r}_{12}$, let us solve for v, the point of intersection. In a procedure similar

to that used in finding the center of the gravisphere, write the intercept point in the form of a displacement along $\bar{r}_{12}$ from μ_1:

$$\bar{r}_{1v} = V\bar{r}_{12} \tag{21}$$

where V is the fraction to be determined. The vector from v to the spacecraft is

$$\bar{r}_{vs} = \bar{r}_{1s} - V\,\bar{r}_{12}$$

Substituting from Eqns. (18) and (19) gives

$$\bar{r}_{vs} = r_{12}\left[\frac{\rho}{1-\rho^2}\,\bar{n} - \left(\frac{\rho^2}{1-\rho^2} + V\right)\,\bar{u}\right] \tag{22}$$

The condition that the relative position vector defined by Eqn. (22 be anti-parallel to the acceleration given by Eqn. (20) is

$$0 = \bar{A}_R \times \bar{r}_{vs}$$

$$= -\frac{r_{12}^2}{(1-\rho^2)r_{2s}^3}\left[\left(\frac{\mu_1}{\rho^2} + \mu_2\rho\right)\,\bar{n} - \left(\frac{\mu_1}{\rho} + \mu_2\right)\,\bar{u}\right] \times \left[\frac{\rho}{1-\rho^2}\,\bar{n} - \left(\frac{\rho^2}{1-\rho^2} + V\right)\,\bar{u}\right]$$

$$= -\frac{r_{12}^2}{(1-\rho^2)r_{2s}^3}\left[\left(\frac{\rho^2}{1-\rho^2} + V\right)\left(\frac{\mu_1}{\rho^2} + \mu_2\rho\right) - \frac{\rho}{1-\rho^2}\left(\frac{\mu_1}{\rho} + \mu_2\right)\right]\,\bar{u} \times \bar{n}$$

Since there must always be an intercept point and since r_{12} and $\bar{u} \times \bar{n}$ in general are not zero, the only alternative is that the

expression in the brackets must be zero. Solving this expression for V gives

$$V = \frac{\mu_2 \rho^3}{\mu_1 + \rho^3 \mu_2}$$

Substituting into Eqn. (21)

$$\bar{r}_{1v} = \frac{\rho^3 \mu_2 \bar{r}_{12}}{\mu_1 + \rho^3 \mu_2} \tag{23}$$

and transforming to the inertial base frame

$$\bar{r}_v = \bar{r}_1 + \bar{r}_{1v} = \frac{\mu_1 \bar{r}_1 + \rho^3 \mu_2 \bar{r}_2}{\mu_1 + \rho^3 \mu_2}$$

Finally, substituting from Eqn. (11) for ρ yields

$$\bar{r}_v = \frac{\frac{\mu_1 \bar{r}_1}{r_{1s}^3} + \frac{\mu_2 \bar{r}_2}{r_{2s}^3}}{\frac{\mu_1}{r_{1s}^3} + \frac{\mu_2}{r_{2s}^3}} \tag{24}$$

Note that, since V and hence $\bar{r}_{1v}$ and $\bar{r}_v$ do not depend upon $\bar{n}$, the intercept point on the vector $\bar{r}_{12}$ is the same for all spacecraft positions on any given gravisphere ρ = constant. Thus, we call this unique fixed point the "gravispheric force center". The mass which would have to be concentrated at v to produce the same gravitational acceleration as μ_1 and μ_2 together is obtained from the equation

$$-\frac{\mu_v \bar{r}_{vs}}{r_{vs}^3} = \bar{A}_R = -\frac{\mu_1(\bar{r}_s-\bar{r}_1)}{r_{1s}^3} - \frac{\mu_2(\bar{r}_s-\bar{r}_2)}{r_{2s}^3}$$

Making use of Eqn. (24), the right side can be expressed in the form

$$\bar{A}_R = -\bar{r}_{vs}\left(\frac{\mu_1}{r_{1s}^3} + \frac{\mu_2}{r_{2s}^3}\right)$$

Hence, μ_v must be

$$\mu_v = r_{vs}^3\left(\frac{\mu_1}{r_{1s}^3} + \frac{\mu_2}{r_{2s}^3}\right) \tag{25}$$

Unlike the force center location, the mass magnitude given by Eqn. (25) is not fixed for all points on a gravisphere. There is rotational symmetry about the $\bar{r}_{12}$ axis, but the magnitude depends upon the displacement from v.

It is of interest to examine the gravispheric force center behavior corresponding to the purely geometric characteristics explored earlier. When $\rho = 0$ and $r_{1s} = 0$, Eqn. (24) shows that $\bar{r}_v = \bar{r}_1$. This, of course, means that $r_{vs} = r_{1s}$ and Eqn. (25) gives $\mu_v = \mu_1$. Similar behavior is noted when $\rho \to \infty$ or $r_{2s} \to 0$: the gravispheric force center goes to $\bar{r}_2$ and the magnitude approaches μ_2. At the halfway plane $\rho = 1$, $r_{1s} = r_{2s}$ and Eqn. (24) reduces to the standard definition for the center of mass. Note, however, that Eqn. (25) does not concentrate the total of μ_1 and μ_2 at v in this case.

2.3 Generalization to More than Two Mass Points

There is no way to extend the preceding concepts to more than two gravitating bodies if one is constrained to the

idea of a gravisphere-like surface of constant distance ratios. There just are no such surfaces or space curves except for very special configurations of mass points. However, the simpler geometry of the gravispheric force center, on the line between a pair of mass points, is easily extendable. Consider the mass configuration in Fig. 3. First select any two mass points, say μ_1 and μ_2. These two can be thought of as being replaced by the gravispheric force center $\mu_{v_{12}}$ appropriate to the spacecraft position relative to them. Next take this fictitious mass $\mu_{v_{12}}$ and another of the real gravitating bodies (μ_3, say) and replace them by their gravispheric force center $\mu_{v_{123}}$ Continue this process, each time taking another one of the unaccounted for real bodies, until they have all been replaced by a single fictitious mass μ_v.

This geometric description can be expressed analytically by straightforward application of Eqns. (24) and (25). The first step yields

$$\left.\begin{aligned} \bar{r}_{v_{12}} &= \frac{\dfrac{\mu_1 \bar{r}_1}{r_{1s}^3} + \dfrac{\mu_2 \bar{r}_2}{r_{2s}^3}}{\dfrac{\mu_1}{r_{1s}^3} + \dfrac{\mu_2}{r_{2s}^3}} \\ \mu_{v_{12}} &= \left(r_{v_{12}s}\right)^3 \left(\frac{\mu_1}{r_{1s}^3} + \frac{\mu_2}{r_{2s}^3}\right) \end{aligned}\right\}$$

where the subscripts 12 indicate that these values account for masses μ_1 and μ_2. Again apply the basic formulas, treating $\mu_{v_{12}}$ as μ_1, $\bar{r}_{v_{12}}$ as $\bar{r}_1$, and μ_3 as μ_2, $\bar{r}_3$ as $\bar{r}_2$:

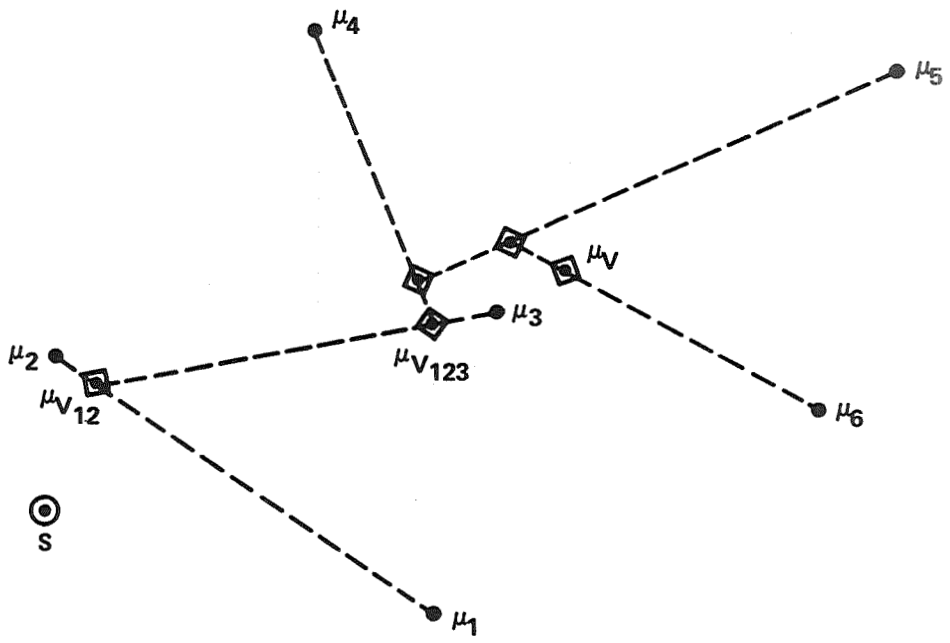

FIGURE 3 - VIRTUAL MASS GEOMETRY

$$\bar{r}_{v_{123}} = \frac{\frac{\mu_{v_{12}}\bar{r}_{v_{12}}}{r_{v_{12}s}^3} + \frac{\mu_3\bar{r}_3}{r_{3s}^3}}{\frac{\mu_{v_{12}}}{r_{v_{12}s}^3} + \frac{\mu_3}{r_{3s}^3}}$$

$$= \frac{\frac{\mu_1\bar{r}_1}{r_{1s}^3} + \frac{\mu_2\bar{r}_2}{r_{2s}^3} + \frac{\mu_3\bar{r}_3}{r_{3s}^3}}{\frac{\mu_1}{r_{1s}^3} + \frac{\mu_2}{r_{2s}^3} + \frac{\mu_3}{r_{3s}^3}}$$

$$\mu_{v_{123}} = r_{v_{123}s}^3 \left(\frac{\mu_{v_{12}}}{r_{v_{12}s}^3} + \frac{\mu_3}{r_{3s}^3}\right)$$

$$= r_{v_{123}s}^3 \left(\frac{\mu_1}{r_{1s}^3} + \frac{\mu_2}{r_{2s}^3} + \frac{\mu_3}{r_{3s}^3}\right)$$

With repeated application of the procedure, one obtains for n attractive bodies:

$$\left.\begin{aligned} \bar{r}_v &= \frac{\bar{M}}{S} \\ \mu_v &= r_{vs}^3 \, S \end{aligned}\right\} \qquad (26)$$

where

$$\bar{M} = \sum_{i=1}^{n} \frac{\mu_i \bar{r}_i}{r_{is}^3}$$

$$S = \sum_{i=1}^{n} \frac{\mu_i}{r_{is}^3}$$

and the definitions of the other terms are the same as given for Eqns. (1). Equations (26) represent the generalization of the gravispheric force center for two masses to the case of n bodies. Since the concept of the gravisphere itself is inappropriate for the larger number of mass points, this generalized effective force center is called the "Virtual Mass". Equations (26) can be differentiated to give the mass rate and velocity of the Virtual Mass as functions of the positions and velocities of the spacecraft and the gravitating bodies:

$$\left.\begin{aligned} \dot{\bar{r}}_v &= \frac{\dot{\bar{M}} - \bar{r}_v \dot{S}}{S} \\ \dot{\mu}_v &= \mu_v \left(\nu_{vs} + \frac{\dot{S}}{S} \right) \end{aligned}\right\} \qquad (27)$$

where

$$\dot{\bar{M}} = \sum_{i=1}^{n} \frac{\mu_i}{r_{is}^3} \left(\dot{\bar{r}}_i - \nu_{is} \bar{r}_i \right)$$

$$\dot{S} = - \sum_{i=1}^{n} \frac{\mu_i}{r_{is}^3} \nu_{is}$$

$$\nu_{is} = \frac{3\dot{\bar{r}}_{is} \cdot \bar{r}_{is}}{r_{is}^2} = \frac{3\dot{r}_{is}}{r_{is}}$$

The uniqueness of the Virtual Mass is evident from Eqns. (26). Any arbitrary ordering of the terms in those equations, corresponding to random sequencing of the mass points of the system, preserves the same values. In the same vein, it is obvious that Virtual Mass replacement of completely arbitrary subgroupings of the n points is permissible. Consider a subgroup of mass points numbered 1 through j, where $j < n$. Equations (26) can be written

$$\left.\begin{aligned} \bar{r}_{v_n} &= \frac{\bar{M}_j + \bar{M}_{n-j}}{S_j + S_{n-j}} \\ \mu_{v_n} &= r_{v_n s}^3 \left(S_j + S_{n-j} \right) \end{aligned}\right\} \qquad (28)$$

where the subscripts n, j, and n-j, respectively, denote mass point groupings of all n bodies, the 1 through j subgroup, and the j + 1 through n remaining subgroup. Inversion of Eqns. (26) to solve for $\bar{M}$ and S shows that

$$\left.\begin{aligned} S &= \frac{\mu_v}{r_{vs}^3} \\ \bar{M} &= \frac{\mu_v \bar{r}_v}{r_{vs}^3} \end{aligned}\right\} \tag{29}$$

Substituting these into Eqn. (28) for the 1 through j subgroup terms and writing out the original definitions of $\bar{M}_{n-j}$ and S_n-j gives

$$\left.\begin{aligned} \bar{r}_{v_n} &= \frac{\dfrac{\mu_{v_j}\bar{r}_{v_j}}{r_{v_j s}^3} + \sum_{i=j+1}^{n} \dfrac{\mu_i \bar{r}_i}{r_{is}^3}}{\dfrac{\mu_{v_j}}{r_{v_j s}^3} + \sum_{i=j+1}^{n} \dfrac{\mu_i}{r_{is}^3}} \\ \mu_{v_n} &= r_{v_n s}^3 \left[\frac{\mu_{v_j}}{r_{v_j s}^3} + \sum_{i=j+1}^{n} \frac{\mu_i}{r_{is}^3}\right] \end{aligned}\right\} \tag{30}$$

Equations (30) clearly show that a subgroup can be replaced by its Virtual Mass relative to the spacecraft, and that this fictitious point can be treated in the same manner as the remaining real bodies to compute the complete system Virtual Mass. This important property will be found quite useful later.

The equivalence of the spacecraft acceleration due to the fictitious mass located at the gravispheric force center

with the acceleration due to the two real mass points was evident in the derivations in Section 2.2. A similar equivalence of the acceleration due to the Virtual Mass with that due to all n real bodies could be argued on the basis of an appropriate superposition principle. However, this is neither necessary nor desirable, since a simple direct proof is possible. The spacecraft equation of motion, Eqn. (1a), can be written

$$\ddot{\bar{r}}_s = - \bar{r}_s \sum_{i=1}^{n} \frac{\mu_i}{r_{is}^3} + \sum_{i=1}^{n} \frac{\mu_i \bar{r}_i}{r_{is}^3}$$

Substituting the definitions used in Eqns. (26):

$$\ddot{\bar{r}}_s = - S\bar{r}_s + \bar{M}$$

and finally introducing the Virtual Mass quantities for S and $\bar{M}$ from Eqns. (29) gives

$$\ddot{\bar{r}}_s = - \frac{\mu_v}{r_{vs}^3} (\bar{r}_s - \bar{r}_v) = - \frac{\mu_v}{r_{vs}^3} \bar{r}_{vs} \qquad (31)$$

The Virtual Mass indeed produces the correct acceleration, and Eqn. (31) is the spacecraft equation of motion in terms of this quantity. Methods of solving this equation will be discussed in the next chapter. First, however, some characteristics of the Virtual Mass will be described.

2.4 Virtual Mass Characteristics

Equations (26) reveal that the Virtual Mass is a variation of the conventional definition of the center of mass of a system of particles. In the position relationship the difference from the usual center of mass lies in the multiplication of the individual masses by a spacecraft proximity weighting factor r_{is}^{-3}. The mass magnitude differs from the

total mass by the application of a weighting factor $\left(r_{vs}/r_{is}\right)^3$ to each term in the summation. As the spacecraft and celestial bodies move, these differences vary the position and magnitude of the fictitious mass in such a way as to produce the correct instantaneous resultant acceleration of the spacecraft.

In the previous discussion of the gravispheric force center it was seen that, for the restricted three body problem, the Virtual Mass position coincides with the center of mass (barycenter) whenever the spacecraft lies on the halfway plane. In particular, for the special case where the spacecraft is in a triangular libration point orbit, the vehicle stays on this plane ($\rho = 1$), and hence the Virtual Mass remains fixed at the center of mass and fixed in magnitude. This is true even in the case of elliptic three body motion. Although the scale changes as a function of time, it does so in such a manner as to preserve the relative geometric similarity. Equations (26) show that as long as the distance ratios remain the same, the Virtual Mass stays constant.

The most general type of trajectory of interest, however, carries the vehicle successively near different celestial bodies. Whenever the spacecraft is near a particular body (e.g., the $k^{\underline{th}}$ one), Eqns. (26) show that that body's contribution to the Virtual Mass position and magnitude is heavily weighted due to division by the relatively small r_{ks}^3. In such a situation, the Virtual Mass is near the dominant celestial body ($\bar{r}_v \approx \bar{r}_k$) and essentially matches it in mass ($\mu_v \approx \mu_k$). Slight differences occur due to the perturbing influences of the other bodies. As the trajectory carries the spacecraft far away from the $k^{\underline{th}}$ body and under the dominant influence of another (call it ℓ), the Virtual Mass moves continuously to the vicinity of the new body and changes to nearly its mass:

$$\left.\begin{aligned} \bar{r}_v \approx \bar{r}_k &\rightarrow \bar{r}_\ell \\ \mu_v \approx \mu_k &\rightarrow \mu_\ell \end{aligned}\right\}$$

Thus, every spacecraft trajectory in an n-body gravity field has associated with it a phantom trajectory of the related Virtual Mass.

An example of an Earth-to-Mars trajectory is shown in Fig. 4. The motions of the celestial bodies were given by JPL Development Ephemeris No. 19 (Ref. 6). The curves are the projections of the three-dimensional trajectories upon a plane passing through the solar system center of mass and parallel to the mean equator of 1950.0. Time ticks are shown along each of the trajectories (spacecraft, Virtual Mass, Earth, and Mars) at approximately equal position displacements. The very small time increments between neighboring tick marks on the Virtual Mass trajectory qualitatively indicate the high inertial velocities achieved in the transition regions (e.g., 0.32 Astronomical Units/day at t = 218 days). To the scale of the plot, the Virtual Mass appears to coincide with the neighboring planetary mass whenever the spacecraft flies by in the near vicinity. Figure 5 shows the corresponding variation of the Virtual Mass magnitude with time. Again, the very rapid changes in the transition regions and the essential equivalence with the currently dominant celestial body are obvious.

2.5 Criterion for Degeneration to Center of Mass

This chapter is concluded with a discussion of the nature of the Virtual Mass when the spacecraft is separated from a group of gravitating mass points by a distance which is large compared with the diameter of the system of masses. By inspection of Eqns. (26) it is seen that, as the ratios of the r_{is}'s to one another and to r_{vs} approach unity, the Virtual Mass equations reduce, in the limit, to the standard forms for the total mass concentrated at the center of mass. It is not anticipated that there will be much interest in spacecraft trajectories which carry to such great distances compared with the size of the solar system as a whole. However, as noted in Section 2.3, a Virtual Mass may be computed for a subgroup of masses and later combined with other subgroup Virtual Masses or with other real bodies. For example, as the spacecraft recedes from Earth on an interplanetary mission, it would be convenient to combine the Earth and Moon as a single mass at their barycenter after the spacecraft is sufficiently far away. Another even more important application will be described in Chapter 4. The crux of the problem then is: Quantitatively, how far is far enough for a prescribed precision of calculation?

Since it has been shown that arbitrary subgroupings are permissible in the calculation of the Virtual Mass, a criterion will be derived for essential correspondence of the Virtual Mass with the center of mass for the case of two gravitating bodies. The application of this criterion when there are more mass points will be discussed in Chapter 4.

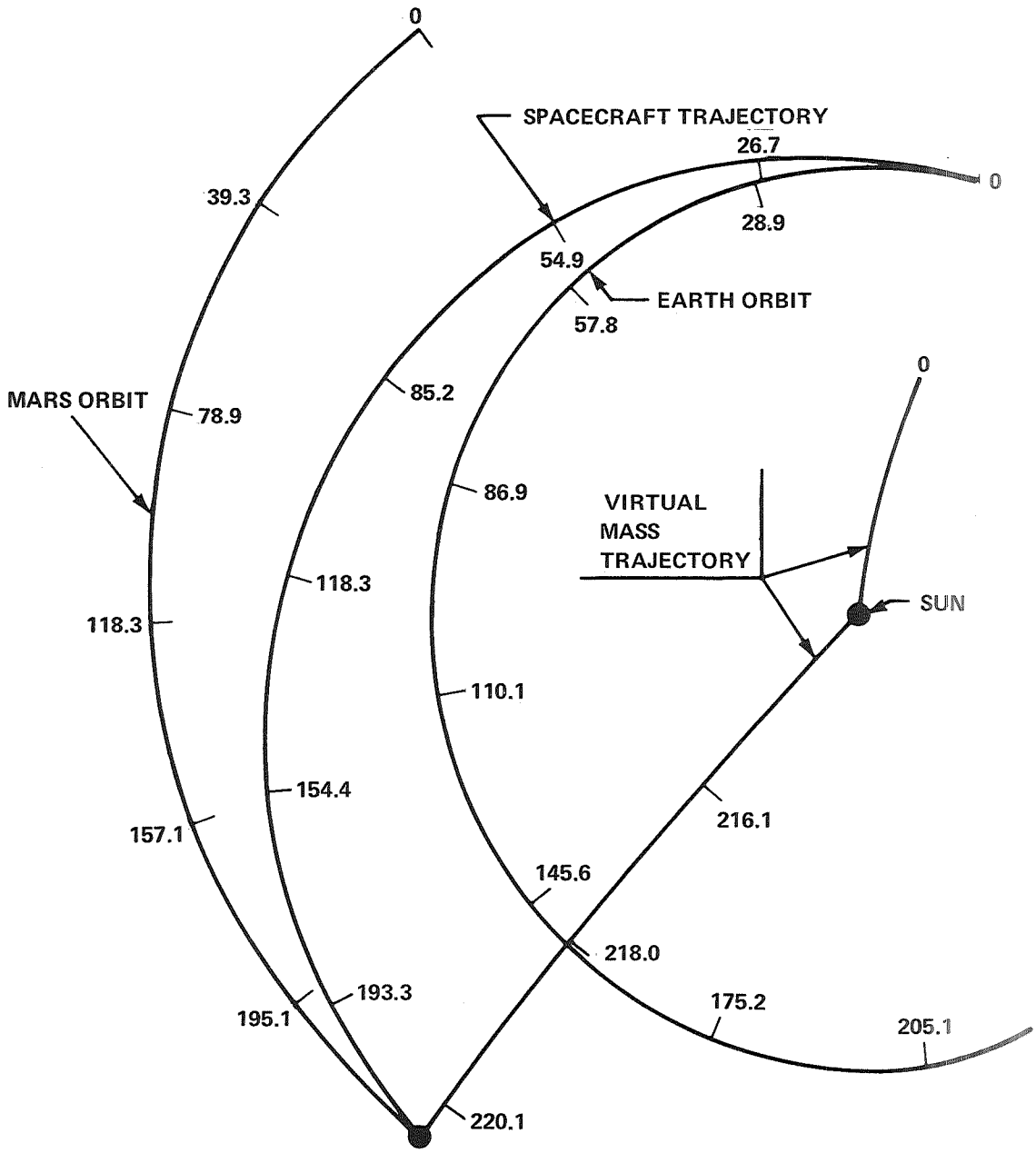

FIGURE 4 - EXAMPLE 221 DAY EARTH-TO-MARS TRAJECTORY, SHOWING PLANETARY AND VIRTUAL MASS TRAJECTORIES

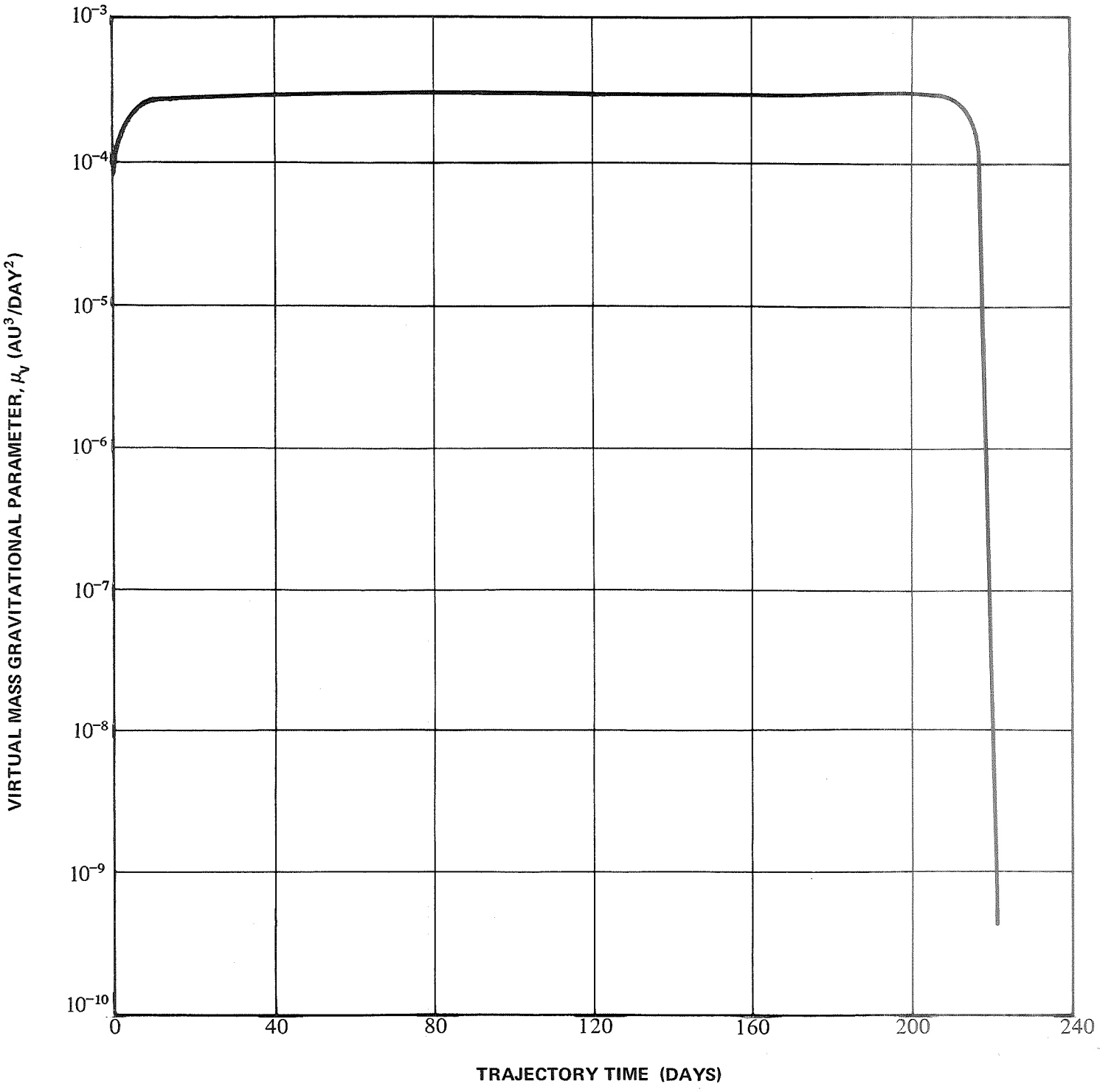

FIGURE 5 - VIRTUAL MASS GRAVITATIONAL PARAMETER VERSUS TIME ALONG EXAMPLE EARTH-TO-MARS TRAJECTORY

The center of mass and the Virtual Mass (gravispheric force center) are known to lie on the line connecting the two mass points. We will simply write an expression for the displacement between them in terms of the parameters describing the spacecraft relative geometry. The vector from the center of mass to the Virtual Mass can be written in terms of the difference of the vectors relative to mass μ_1:

$$\bar{r}_{cv} = \bar{r}_{1v} - \bar{r}_{1c} \tag{32}$$

where obviously

$$\bar{r}_{1c} = \frac{\mu_2}{\mu_1 + \mu_2} \bar{r}_{12} \tag{33}$$

Substituting Eqns. (23) and (33) into Eqn. (32) gives

$$\bar{r}_{cv} = \left(\frac{\rho^3 \mu_2}{\mu_1 + \rho^3 \mu_2} - \frac{\mu_2}{\mu_1 + \mu_2} \right) \bar{r}_{12} \tag{34}$$

We now proceed to express ρ in a form convenient for our purpose. First write $\bar{r}_{1s}$ and $\bar{r}_{2s}$ in terms of the spacecraft position $\bar{r}_{cs}$ relative to the center of mass:

$$\left.\begin{aligned} \bar{r}_{1s} &= \bar{r}_{cs} + \bar{r}_{1c} = \bar{r}_{cs} + \frac{\mu_2}{\mu_1 + \mu_2} \bar{r}_{12} \\ \bar{r}_{2s} &= \bar{r}_{cs} + \bar{r}_{2c} = \bar{r}_{cs} - \frac{\mu_1}{\mu_1 + \mu_2} \bar{r}_{12} \end{aligned}\right\}$$

and then compute

$$r_{1s}^2 = \bar{r}_{1s}\cdot\bar{r}_{1s} = r_{cs}^2 + \left(\frac{\mu_2}{\mu_1 + \mu_2}\right)^2 r_{12}^2 + \frac{2\mu_2}{\mu_1 + \mu_2}\,\bar{r}_{cs}\cdot\bar{r}_{12}$$

$$r_{2s}^2 = \bar{r}_{2s}\cdot\bar{r}_{2s} = r_{cs}^2 + \left(\frac{\mu_1}{\mu_1 + \mu_2}\right)^2 r_{12}^2 - \frac{2\mu_1}{\mu_1 + \mu_2}\,\bar{r}_{cs}\cdot\bar{r}_{12}$$

Factoring out r_{cs}^2 and writing

$$\frac{r_{12}}{r_{cs}} \triangleq \varepsilon \tag{35}$$

one obtains

$$\left.\begin{aligned} r_{1s}^2 &= r_{cs}^2\left[1 + \left(\frac{\mu_2}{\mu_1 + \mu_2}\right)^2 \varepsilon^2 + \frac{2\mu_2}{\mu_1 + \mu_2}\,\varepsilon\cos\theta\right] \\ r_{2s}^2 &= r_{cs}^2\left[1 + \left(\frac{\mu_1}{\mu_1 + \mu_2}\right)^2 \varepsilon^2 - \frac{2\mu_1}{\mu_1 + \mu_2}\,\varepsilon\cos\theta\right] \end{aligned}\right\} \tag{36}$$

where θ is the angle between $\bar{r}_{cs}$ and $\bar{r}_{12}$. Since we are interested in the case where the spacecraft displacement is large compared with the distance between the two mass points, ε is a small parameter and terms higher than first order in ε will be neglected. This approximation in Eqn. (36) results in

$$\rho^2 = \frac{r_{1s}^2}{r_{2s}^2} = \frac{1 + \dfrac{2\mu_2}{\mu_1 + \mu_2}\,\varepsilon\cos\theta}{1 - \dfrac{2\mu_1}{\mu_1 + \mu_2}\,\varepsilon\cos\theta}$$

Again, assuming the second term is small compared with unity:

$$\rho^2 = \left(1 + \frac{2\mu_2}{\mu_1 + \mu_2}\,\varepsilon\cos\theta\right)\left(1 + \frac{2\mu_1}{\mu_1 + \mu_2}\,\varepsilon\cos\theta\right)$$

$$= 1 + 2\varepsilon\cos\theta$$

to first order in ε. Since the real interest is in the cube, not the square of ρ:

$$\rho^3 = (1 + 2\varepsilon\cos\theta)^{3/2} \approx 1 + 3\varepsilon\cos\theta \qquad (37)$$

Finally, substituting Eqn. (37) into Eqn. (34) and simplifying gives

$$\bar{r}_{cv} = \frac{3\mu_1\mu_2}{(\mu_1 + \mu_2)^2}\,\varepsilon\cos\theta\;\bar{r}_{12}$$

The vector magnitude is the only quantity of interest; thus

$$r_{cv} = \frac{3\mu_1\mu_2}{(\mu_1 + \mu_2)^2}\,\varepsilon\cos\theta\;r_{12}$$

The maximum displacement of the Virtual Mass from the mass center occurs when $|\cos\theta| = 1$. Thus, $\cos\theta$ is set equal to 1 for a worst case analysis. Substituting for ε from Eqn. (35) and dividing through the equation by r_{cs}:

$$\frac{r_{cv}}{r_{cs}} = \frac{3\mu_1\mu_2}{(\mu_1 + \mu_2)^2}\,\frac{r_{12}^2}{r_{cs}^2}$$

Treating the ratio on the left as a prescribed precision which is desired, this equation can be solved for the spacecraft distance beyond which the two mass points can be coalesced at the center of mass:

$$r_{cs} = \frac{r_{12}}{\mu_1 + \mu_2}\sqrt{\frac{3\mu_1\mu_2}{r_{cv}/r_{cs}}} = \sqrt{\frac{3r_{c1}r_{c2}}{r_{cv}/r_{cs}}} \tag{38}$$

3.0 CALCULATION OF NUMERICAL SOLUTIONS USING THE VIRTUAL MASS

3.1 Mathematical Considerations

It was shown in Eqn. (31) of the preceding chapter that the Virtual Mass replaces the combined gravitational effects of all the celestial bodies acting upon the spacecraft. This equation, repeated here,

$$\ddot{\bar{r}}_s = -\frac{\mu_v \bar{r}_{vs}}{r_{vs}^3} \tag{39}$$

looks deceptively simple. Although it does reduce the problem to a two-body case, there is no general solution for it. The most obvious difficulty occurs because of the non-constancy of μ_v, the Virtual Mass magnitude. In addition, the acceleration of the spacecraft on the left is with respect to a Newtonian inertial frame, whereas the spacecraft position vector on the right is measured relative to the accelerating Virtual Mass. Writing

$$\left.\begin{aligned} \bar{r}_s &= \bar{r}_{vs} + \bar{r}_v \\ \dot{\bar{r}}_s &= \dot{\bar{r}}_{vs} + \dot{\bar{r}}_v \\ \ddot{\bar{r}}_s &= \ddot{\bar{r}}_{vs} + \ddot{\bar{r}}_v \end{aligned}\right\} \tag{40}$$

where the single subscript v denotes measurement of the Virtual Mass quantity with respect to the inertial frame, Eqn. (39) becomes

$$\ddot{\bar{r}}_{vs} = - \frac{\mu_v \bar{r}_{vs}}{r_{vs}^3} - \ddot{\bar{r}}_v \qquad (41)$$

As noted, no general integral exists; hence, one must resort to numerical procedures in order to obtain approximate solutions. The simplest approach, defined conceptually in the Introduction, involves exact solutions of approximations to the equation of motion, Eqn. (41). Three such techniques are reported in Ref. 3.

The least sophisticated can be characterized as a simple Euler procedure. Here the Virtual Mass magnitude and inertial position are held constant at the values corresponding to the beginning of the computing interval. Thus

$$\ddot{\bar{r}}_v = 0, \quad \ddot{\bar{r}}_{vs} = \ddot{\bar{r}}_s \text{ and } \mu_v = \mu_{v_o} = \text{constant}$$

and Eqns. (39) or (41) reduce to the classical two body case for which the conic section solution applies. The initial conditions of position and velocity are

$$\left.\begin{aligned} \bar{r}_{vs_o} &= \bar{r}_{s_o} - \bar{r}_{v_o} \\ \dot{\bar{r}}_{vs_o} &= \dot{\bar{r}}_{s_o} \end{aligned}\right\}$$

since $\dot{\bar{r}}_{v_o}$ is taken as zero. Even with very small computing intervals, this procedure diverges quite rapidly from the true solution.

An obvious improvement in this simple Euler method would be afforded by considering a better representation of the motion of the Virtual Mass. In this case the magnitude would again be held constant at the initial value, $\mu_v = \mu_{v_o} = \text{constant}$. However, the position would be allowed

to change from the initial value $\bar{r}_{v_o}$ at the constant velocity $\dot{\bar{r}}_{v_o}$. Clearly it would still be true that $\ddot{\bar{r}}_v = 0$ and $\ddot{\bar{r}}_{vs} = \ddot{\bar{r}}_s$; hence, the classical two body solution would again be valid for the relative motion. The initial conditions would be $\bar{r}_{vs_o}$, $\dot{\bar{r}}_{vs_o}$ and the final spacecraft inertial state would be obtained from

$$\left.\begin{aligned} \bar{r}_s &= \bar{r}_{vs} + \bar{r}_{v_o} + \dot{\bar{r}}_{v_o}\ (\delta t) \\ \dot{\bar{r}}_s &= \dot{\bar{r}}_{vs} + \dot{\bar{r}}_{v_o} \end{aligned}\right\}$$

where δt is the computation time interval. This method shows marked improvement over the first, but still diverges faster than desired from the correct solution.

The best method in this category is a modified Euler technique considering relative motion. Here the assumptions regarding the Virtual Mass time history are precisely the same as for the immediately preceding case. The difference is that an average mass value and an average velocity are held over the interval. The values used are

$$\left.\begin{aligned} \mu_{v_{av}} &= \frac{\mu_{v_o} + \mu_v}{2} \\ \dot{\bar{r}}_{v_{av}} &= \frac{\bar{r}_v - \bar{r}_{v_o}}{\delta t} \end{aligned}\right\}$$

and obviously necessitate an iterative computation procedure to determine compatible sets of values of average and final values.

Despite the fact the conic section solution itself has to be included in the iteration cycle (because of the changing mass and initial velocity), this method significantly

outperforms the other two in terms of speed and accuracy. The details are reported in Ref. 3. The best accuracy achievable, however, is limited to holding the restricted three-body Jacobi energy to a variation of 2 parts out of 7×10^6 for a typical free-return Earth-to-Moon transfer trajectory. This accuracy is adequate for the calculation of lunar trajectories, but not for precision interplanetary work. In addition, this general approach to obtaining solutions has difficulty in handling non-gravitational accelerations such as rocket thrust, solar radiation pressure, aerodynamic forces, etc. Consequently, we turn in this memorandum to the category of solution methods comprising the approximate solutions of the exact equations of motion.

First, for the sake of complete generality, add the term $\bar{a}$ to Eqns. (39) and (41) to include any and all accelerations other than point mass gravitational terms:

$$\ddot{\bar{r}}_s = - \frac{\mu_v \bar{r}_{vs}}{r_{vs}^3} + \bar{a} \tag{42}$$

$$\ddot{\bar{r}}_{vs} = - \frac{\mu_v \bar{r}_{vs}}{r_{vs}^3} - \ddot{\bar{r}}_v + \bar{a} \tag{43}$$

Following the Encke approach, let us introduce a reference conic solution which can be computed exactly. The difference between this and the complete solution is the perturbation solution and this is the part to be calculated by an approximate procedure. As in the classical Encke method, it is assumed that the reference trajectory is a conic section two-body solution. However, the Virtual Mass is selected as the reference body, rather than one of the real celestial bodies. Thus, the solution to Eqn. (43) is represented as

$$\bar{r}_{vs} = \bar{r}_{vr} + \bar{r}_{rs} \tag{44}$$

where $\bar{r}_{vr}$ is the reference conic relative to the Virtual Mass and $\bar{r}_{rs}$ is the perturbation from the reference conic to the

true spacecraft trajectory. The differential equation defining the two-body reference conic is

$$\ddot{\bar{r}}_{vr} = - \frac{\mu_{v_o} \bar{r}_{vr}}{r_{vr}^3} \tag{45}$$

where μ_{v_o} is held constant at the Virtual Mass magnitude at the beginning of the computing interval. The initial conditions

$$\left.\begin{aligned} \bar{r}_{vr_o} &= \bar{r}_{vs_o} \\ \dot{\bar{r}}_{vr_o} &= \dot{\bar{r}}_{vs_o} \end{aligned}\right\} \tag{46}$$

are chosen so the conic section osculates the true solution at the beginning of the interval. The differential equation which must be satisfied by the perturbation term $\bar{r}_{rs}$ is obtained by twice differentiating Eqn. (44) and substituting for $\ddot{\bar{r}}_{vr}$ from Eqn. (45) and for $\ddot{\bar{r}}_{vs}$ from Eqn. (43)

$$\ddot{\bar{r}}_{rs} = \frac{\mu_{v_o} \bar{r}_{vr}}{r_{vr}^3} - \frac{\mu_v \bar{r}_{vs}}{r_{vs}^3} - \ddot{\bar{r}}_v + \bar{a} \tag{47}$$

In view of Eqns. (46) and the definition in Eqn. (44) and its first derivative, we see that the initial conditions for this differential equation are

$$\bar{r}_{rs_o} = \dot{\bar{r}}_{rs_o} = 0 \tag{48}$$

Equation (47) shows clearly that the perturbation term accounts for the accelerated motion of the Virtual Mass, the variability of its magnitude, and the non-point-mass accelerations $\bar{a}$.

Although Eqn. (47) looks quite similar to the perturbation equation associated with the classical Encke procedure, the use of the variable Virtual Mass renders the usual solution methods ineffective. It is true that Eqn. (27a) can be differentiated to obtain an explicit expression for $\ddot{\bar{r}}_v$. However, this is undesirable from two standpoints:

(1) The algebra is complicated; hence, it offers no real help in trying to solve Eqn. (47).

(2) The expression explicitly involves $\ddot{\bar{r}}_s$ and $\ddot{\bar{r}}_i$. These can be eliminated by substituting from Eqns. (1), but the algebra becomes even worse and the complete system of differential equations is reintroduced.

One obvious way around the difficulty is to expand $\bar{r}_{rs}$ and $\bar{r}_v$ in a Taylor's series

$$\left.\begin{aligned} \bar{r}_{rs} &= \bar{r}_{rs_o} + \dot{\bar{r}}_{rs_o}(\delta t) + \frac{1}{2}\ddot{\bar{r}}_{rs_o}(\delta t)^2 + \frac{1}{6}\dddot{\bar{r}}_{rs_o}(\delta t)^3 + \cdots \\ \bar{r}_v &= \bar{r}_{v_o} + \dot{\bar{r}}_{v_o}(\delta t) + \frac{1}{2}\ddot{\bar{r}}_{v_o}(\delta t)^2 + \frac{1}{6}\dddot{\bar{r}}_{v_o}(\delta t)^3 + \cdots \end{aligned}\right\} \quad (49)$$

if the coefficients can be evaluated conveniently. Assuming that an iterative computation procedure will be employed, we may consider that the Virtual Mass position and velocity are given by Eqns. (26) and (27) at the beginning and end of the interval δt (the end values are the ones to be iteratively improved). Thus, Eqn. (49b) and its derivative,

$$\dot{\bar{r}}_v = \dot{\bar{r}}_{v_o} + \ddot{\bar{r}}_{v_o}(\delta t) + \frac{1}{2}\dddot{\bar{r}}_{v_o}(\delta t)^2, \quad (50)$$

both truncated at the third order terms, can be considered as a system of two equations in the unknowns $\ddot{\bar{r}}_{v_o}$, $\dddot{\bar{r}}_{v_o}$. Explicit solution for these quantities gives

$$\left.\begin{aligned} \ddot{\bar{r}}_{v_o} &= \frac{6(\bar{r}_v - \bar{r}_{v_o}) - 2(2\dot{\bar{r}}_{v_o} + \dot{\bar{r}}_v)(\delta t)}{(\delta t)^2} \\ \dddot{\bar{r}}_{v_o} &= \frac{12(\bar{r}_{v_o} - \bar{r}_v) + 6(\dot{\bar{r}}_{v_o} + \dot{\bar{r}}_v)(\delta t)}{(\delta t)^3} \end{aligned}\right\} \qquad (51)$$

This constant jerk (third derivative) representation of the Virtual Mass is the simplest which still satisfies the exact positions and velocities at the beginning and end of the computing interval.

The evaluation of the coefficients of the expansion in Eqn. (49a) for the perturbation term $\bar{r}_{rs}$ depends on the coefficients just determined in Eqns. (51) and on the definition in Eqn. (47). First, note that the two leading coefficients of Eqn. (49a) vanish by Eqn. (48). The remaining coefficients involve second and higher order derivatives of $\bar{r}_{rs}$, evaluated at the start of the interval. These can be determined by Eqn. (47) and higher order derivatives of it, evaluated at the beginning point. For the sake of notational simplification set

$$\bar{K} \triangleq \frac{\mu_{r_o}\bar{r}_{vr}}{r_{vr}^3} - \frac{\mu_v\bar{r}_{vs}}{r_{vs}^3} \qquad (52)$$

Then Eqn. (47) and its derivatives can be written

$$\left.\begin{aligned} \ddot{\bar{r}}_{rs} &= \bar{K} - \ddot{\bar{r}}_v + \bar{a} \\ \dddot{\bar{r}}_{rs} &= \dot{\bar{K}} - \dddot{\bar{r}}_v + \dot{\bar{a}} \\ \ddddot{\bar{r}}_{rs} &= \ddot{\bar{K}} - \ddddot{\bar{r}}_v + \ddot{\bar{a}} \end{aligned}\right\} \qquad (53)$$

etc.

where, in addition to Eqn. (52), we have

$$\dot{\bar{K}} = \frac{\mu_{V_o}\dot{\bar{r}}_{vr}}{r_{vr}^3} - \frac{3\mu_{V_o}\bar{r}_{vr}}{r_{vr}^4}\left(\dot{\bar{r}}_{vr}\cdot\frac{\bar{r}_{vr}}{r_{vr}}\right) - \frac{\mu_V\dot{\bar{r}}_{vs}}{r_{vs}^3}$$

$$+ \frac{3\mu_V\bar{r}_{vs}}{r_{vs}^4}\left(\dot{\bar{r}}_{vs}\cdot\frac{\bar{r}_{vs}}{r_{vs}}\right) - \frac{\dot{\mu}_V\bar{r}_{vs}}{r_{vs}^3}$$

$$\ddot{\bar{K}} = \frac{\bar{r}_{vr}}{r_{vr}}\left\{\frac{\mu_{V_o}}{r_{vr}^4}\left[\frac{2\mu_{V_o}}{r_{vr}} - 3\left(\dot{\bar{r}}_{vr}\cdot\dot{\bar{r}}_{vr}\right) + 15\left(\dot{\bar{r}}_{vr}\cdot\frac{\bar{r}_{vr}}{r_{vr}}\right)^2\right]\right\}$$

$$- \dot{\bar{r}}_{V_r}\left[\frac{6\mu_{V_o}}{r_{vr}^4}\left(\dot{\bar{r}}_{vr}\cdot\frac{\bar{r}_{vr}}{r_{vr}}\right)\right] + \dot{\bar{r}}_{vs}\left[\frac{6\mu_V}{r_{vs}^4}\left(\dot{\bar{r}}_{vs}\cdot\frac{\bar{r}_{vs}}{r_{vs}}\right) - \frac{2\dot{\mu}_V}{r_{vs}^3}\right] \quad (54)$$

$$- \frac{\bar{r}_{vs}}{r_{vs}}\left\{\frac{\mu_V}{r_{vs}^4}\left[\frac{2\mu_V}{r_{vs}} - 3\left[\dot{\bar{r}}_{vs}\cdot\dot{\bar{r}}_{vs} - \bar{r}_{vs}\cdot\left(\ddot{\bar{r}}_V - \bar{a}\right)\right]\right.\right.$$

$$\left.\left. + 15\left(\dot{\bar{r}}_{vs}\cdot\frac{\bar{r}_{vs}}{r_{vs}}\right)^2\right] - \frac{6\dot{\mu}_V}{r_{vs}^3}\left(\dot{\bar{r}}_{vs}\cdot\frac{\bar{r}_{vs}}{r_{vs}}\right) + \frac{\ddot{\mu}_V}{r_{vs}^2}\right\}$$

$$+ \frac{\mu_V}{r_{vs}^3}\left(\ddot{\bar{r}}_V - \bar{a}\right)$$

etc.

In writing Eqn. (54b) in the form shown, use was made of Eqns. (43) and (45) to eliminate the derivatives $\ddot{\bar{r}}_{vs}$ and $\ddot{\bar{r}}_{vr}$. Note that the substitution of Eqn. (43) introduced the non-gravitational term $\bar{a}$ into this derivative of $\bar{K}$. It is assumed that $\bar{a}$ and its derivatives are known functions. Evaluation of Eqns. (52), (53), and (54) at the beginning of the computation interval gives

$$\left.\begin{aligned}
\bar{K}_o &= 0 \\
\dot{\bar{K}}_o &= -\frac{\dot{\mu}_{v_o}\bar{r}_{vr_o}}{r_{vr_o}^3} \\
\ddot{\bar{K}}_o &= -\frac{\bar{r}_{vr_o}}{r_{vr_o}}\left\{\frac{3\mu_{v_o}}{r_{vr_o}^3}\frac{\bar{r}_{vr_o}}{r_{vr_o}}\cdot\left(\ddot{\bar{r}}_{v_o}-\bar{a}_o\right)-\frac{6\dot{\mu}_{v_o}}{r_{vr_o}^3}\left(\dot{\bar{r}}_{vr_o}\cdot\frac{\bar{r}_{vr_o}}{r_{vr_o}}\right)+\frac{\ddot{\mu}_{v_o}}{r_{vr_o}^2}\right\} \\
&\quad -\frac{2\dot{\mu}_{v_o}\dot{\bar{r}}_{vr_o}}{r_{vr_o}^3}+\frac{\mu_{v_o}}{r_{vr_o}^3}\left(\ddot{\bar{r}}_{v_o}-\bar{a}_o\right)
\end{aligned}\right\} \quad (55)$$

and

$$\ddot{\bar{r}}_{rs_o} = - \ddot{\bar{r}}_{v_o} + \bar{a}_o$$

$$\dddot{\bar{r}}_{rs_o} = - \frac{\dot{\mu}_{v_o} \bar{r}_{vr_o}}{r_{vr_o}^3} - \dddot{\bar{r}}_{v_o} + \dot{\bar{a}}_o$$

$$\ddddot{\bar{r}}_{rs_o} = - \frac{\bar{r}_{vr_o}}{r_{vr_o}} \left\{ \frac{3\mu_{v_o}}{r_{vr_o}^3} \frac{\bar{r}_{vr_o}}{r_{vr_o}} \cdot \left(\ddot{\bar{r}}_{v_o} - \bar{a}_o \right) - \frac{6\dot{\mu}_{v_o}}{r_{vr_o}^3} \left(\dot{\bar{r}}_{vr_o} \cdot \frac{\bar{r}_{vr_o}}{r_{vr_o}} \right) + \frac{\ddot{\mu}_{v_o}}{r_{vr_o}^2} \right\} \qquad (56)$$

$$- \frac{2\dot{\mu}_{v_o} \dot{\bar{r}}_{vr_o}}{r_{vr_o}^3} + \frac{\mu_{v_o}}{r_{vr_o}^3} \left(\ddot{\bar{r}}_{v_o} - \bar{a}_o \right) + \ddot{\bar{a}}_o$$

The derivatives $\ddot{\bar{r}}_{v_o}$ and $\dddot{\bar{r}}_{v_o}$ are given by Eqns. (51). Note that the $\ddddot{\bar{r}}_{v_o}$ term in Eqn. (56c) was eliminated since it is zero in this constant jerk representation of the Virtual Mass motion. The derivative $\ddot{\mu}_{v_o}$ would have to be determined from a Taylor's series expansion for μ_v similar to Eqn. (49b) for $\bar{r}_v$. A scalar solution exactly analogous to Eqns. (51) results for $\ddot{\mu}_{vo}$ and $\dddot{\mu}_{vo}$.

This solution procedure was tested for the case of a fifth order expansion in the correction term $\bar{r}_{rs}$. As might be expected from Eqns. (54), (55) and (56), extension to fifth order involves considerably more complicated algebra, but is otherwise straightforward. The results showed an improved performance over the best method of Ref. 3 -- the modified Euler procedure, considering piecewise uniform motion of the Virtual Mass.

However, the constant jerk restriction of the Virtual Mass representation apparently limits the accuracy improvement to only a couple of orders of magnitude, or about 1 part in 10^8 in the constancy of the Jacobi energy on the test lunar trajectory. Even this accuracy was bought at high expense in terms of running time, since small computing intervals were required. Although a detailed investigation was not conducted, it appears that the chief source of the difficulty lies in the Virtual Mass representation. Indeed, one is hard-pressed to justify a fifth order representation of a perturbative correction when the gross motion of the Virtual Mass is limited to a third order expansion.

Fortunately, the problem is quite easily circumvented, making possible a simple yet highly accurate procedure. The trick lies in treating Eqn. (47) not as the differential equation for the perturbation $\bar{r}_{rs}$ alone, but rather for the combination

$$\bar{r}_c \triangleq \bar{r}_{rs} + \bar{r}_v \tag{57}$$

The realization that this combination should be made comes when one substitutes Eqn. (57) and its derivative into Eqn. (44) and its derivative, and uses that result in Eqns. (40a, b):

$$\left.\begin{aligned} \bar{r}_s &= \bar{r}_{vr} + \bar{r}_c \\ \dot{\bar{r}}_s &= \dot{\bar{r}}_{vr} + \dot{\bar{r}}_c \end{aligned}\right\} \tag{58}$$

Clearly, all one needs is the reference conic and $\bar{r}_c$. Rewriting Eqn. (47) in terms of the definitions in Eqns. (52) and (57) gives for the second order differential equation (for the acceleration) and its next higher derivative (for the jerk):

$$\left.\begin{aligned} \ddot{\bar{r}}_c &= \bar{K} + \bar{a} \\ \dddot{\bar{r}}_c &= \dot{\bar{K}} + \dot{\bar{a}} \end{aligned}\right\} \tag{59}$$

We are not interested in higher order derivatives since, by Eqns. (54), these involve $\ddot{\bar{r}}_V$, $\ddot{\mu}_V$ and higher derivatives which are evaluated only with great difficulty.

Expanding the combined correction solution $\bar{r}_c$ in a Taylor's series yields

$$\bar{r}_c = \bar{r}_{c_o} + \dot{\bar{r}}_{c_o}(\delta t) + \frac{1}{2}\ddot{\bar{r}}_{c_o}(\delta t)^2 + \frac{1}{6}\dddot{\bar{r}}_{c_o}(\delta t)^3 + \frac{1}{24}\ddddot{\bar{r}}_{c_o}(\delta t)^4 + \frac{1}{120}\dddddot{\bar{r}}_{c_o}(\delta t)^5$$

$$\dot{\bar{r}}_c = \dot{\bar{r}}_{c_o} + \ddot{\bar{r}}_{c_o}(\delta t) + \frac{1}{2}\dddot{\bar{r}}_{c_o}(\delta t)^2 + \frac{1}{6}\ddddot{\bar{r}}_{c_o}(\delta t)^3 + \frac{1}{24}\dddddot{\bar{r}}_{c_o}(\delta t)^4 \qquad (60)$$

$$\ddot{\bar{r}}_c = \ddot{\bar{r}}_{c_o} + \dddot{\bar{r}}_{c_o}(\delta t) + \frac{1}{2}\ddddot{\bar{r}}_{c_o}(\delta t)^2 + \frac{1}{6}\dddddot{\bar{r}}_{c_o}(\delta t)^3$$

$$\dddot{\bar{r}}_c = \dddot{\bar{r}}_{c_o} + \ddddot{\bar{r}}_{c_o}(\delta t) + \frac{1}{2}\dddddot{\bar{r}}_{c_o}(\delta t)^2$$

The reason for truncating at the fifth order terms will become apparent. Evaluating Eqn. (57) and its derivative at the beginning of the interval and taking into account Eqn. (48) shows that

$$\left.\begin{aligned} \bar{r}_{c_o} &= \bar{r}_{v_o} \\ \dot{\bar{r}}_{c_o} &= \dot{\bar{r}}_{v_o} \end{aligned}\right\} \qquad (61)$$

These are known by the Virtual Mass definitions in Eqns. (26) and (27). Evaluating Eqn. (59) at the start of the interval and substituting from Eqn. (55), we see that

$$\left.\begin{aligned} \ddot{\bar{r}}_{c_o} &= \bar{K}_o + \bar{a}_o = \bar{a}_o \\ \dddot{\bar{r}}_{c_o} &= \dot{\bar{K}}_o + \dot{\bar{a}}_o = -\frac{\dot{\mu}_{v_o}\bar{r}_{vr_o}}{r_{vr_o}^3} + \dot{\bar{a}}_o \end{aligned}\right\} \qquad (62)$$

This is as far as the coefficient determination can be carried considering conditions only at the start of the computing interval and limiting ourselves to no knowledge of the Virtual Mass derivatives beyond the first. However, additional coefficient determinations can be made if we consider conditions at points other than the beginning of the interval. Specifically, assume that the quantities in Eqns. (59) are evaluated at the end of the computing interval.* The relations in Eqns. (60c, d) are inferred to be evaluated at the end of the interval since δt denotes the total time increment. Equating these two expressions for $\ddot{\bar{r}}_c$, $\dddot{\bar{r}}_c$ and substituting from Eqns. (62) for $\bar{r}_{c_o}$, $\overline{r_{c_o}}$, gives the following two equations in the unknowns $\ddddot{\bar{r}}_{c_o}$, $\overline{\ddddot{r}}_{c_o}$:

$$\left.\begin{aligned} \frac{1}{2}\ddddot{\bar{r}}_{c_o}(\delta t)^2 + \frac{1}{6}\overline{\ddddot{r}}_{c_o}(\delta t)^3 &= \bar{K} + \bar{a} - \bar{K}_o - \bar{a}_o - \left(\dot{\bar{K}}_o + \dot{\bar{a}}_o\right)\delta t \\ \ddddot{\bar{r}}_{c_o}(\delta t) + \frac{1}{2}\overline{\ddddot{r}}_{c_o}(\delta t)^2 &= \dot{\bar{K}} + \dot{\bar{a}} - \dot{\bar{K}}_o - \dot{\bar{a}}_o \end{aligned}\right\}$$

*This of course implies an iteration procedure, since $\bar{K}$ and $\dot{\bar{K}}$ depend upon $\bar{r}_v$, $\dot{\bar{r}}_v$, μ_v and $\dot{\mu}_v$ at the end of the interval, and these have yet to be determined.

Solving these explicitly for the unknowns results in

$$\left.\begin{aligned} \ddddot{\bar{r}}_{c_o} &= \frac{1}{(\delta t)^2}\left[6\,(\bar{K} + \bar{a} - \bar{K}_o - \bar{a}_o) - 2\,(\dot{\bar{K}} + \dot{\bar{a}} + 2\dot{\bar{K}}_o + 2\dot{\bar{a}}_o)\delta t\right] \\ \dddddot{\bar{r}}_{c_o} &= \frac{1}{(\delta t)^3}\left[6(\dot{\bar{K}} + \dot{\bar{a}} + \dot{\bar{K}}_o + \dot{\bar{a}}_o)\delta t + 12(\bar{K}_o + \bar{a}_o - \bar{K} - \bar{a})\right] \end{aligned}\right\} \quad (63)$$

Finally, substituting Eqns. (52), (54) and (55) into Eqn. (63); then Eqns. (61), (62) and (63) into Eqns. (60 a, b); and then this result into Eqns. (58) leads to the iteration equations for the final spacecraft state:

$$\left.\begin{aligned} \bar{r}_s &= \bar{X}_o + \bar{X} \\ \dot{\bar{r}}_s &= \dot{\bar{X}}_o + \dot{\bar{X}} \end{aligned}\right\} \quad (64)$$

where the definitions of the terms on the right are

$$\bar{X}_o = \bar{r}_{v_o} + \dot{\bar{r}}_{v_o}(\delta t) + \frac{7}{20}\bar{a}_o(\delta t)^2 - \frac{\dot{\mu}_{v_o}\bar{r}_{vr_o}}{20 r_{vr_o}^3}(\delta t)^3 + \frac{\dot{\bar{a}}_o}{20}(\delta t)^3$$

$$+ \bar{r}_{vr}\left\{1 + \frac{(\delta t)^2}{20}\frac{\mu_{v_o}}{r_{vr}^3}\left[3 + 2\left(\frac{\dot{\bar{r}}_{vr}}{r_{vr}}\cdot\frac{\bar{r}_{vr}}{r_{vr}}\right)\delta t\right]\right\} - \frac{(\delta t)^3}{30}\frac{\mu_{v_o}\dot{\bar{r}}_{vr}}{r_{vr}^3}$$

$$\dot{\bar{X}}_o = \dot{\bar{r}}_{v_o} + \frac{\bar{a}_o}{2}(\delta t) - \frac{\dot{\mu}_{v_o}\bar{r}_{vr_o}}{12 r_{vr_o}^3}(\delta t)^2 + \frac{\dot{\bar{a}}_o}{12}(\delta t)^2$$

$$+ \frac{\delta t}{4}\frac{\mu_{v_o}}{r_{vr}^3}\left[2 + \delta t\left(\frac{\dot{\bar{r}}_{vr}}{r_{vr}}\cdot\frac{\bar{r}_{vr}}{r_{vr}}\right)\right]\bar{r}_{vr} + \left[1 - \frac{\mu_{v_o}}{r_{vr}^3}\frac{(\delta t)^2}{12}\right]\dot{\bar{r}}_{vr}$$

Cont.

$$\dot{\bar{X}} = \frac{\delta t}{4}\left\{\frac{\delta t}{3}\frac{\dot{\mu}_V}{r_{vs}^3} - \frac{\mu_V}{r_{vs}^3}\left[2 + \left(\frac{\dot{\bar{r}}_{vs}}{r_{vs}}\cdot\frac{\bar{r}_{vs}}{r_{vs}}\right)\delta t\right]\right\}\bar{r}_{vs} + \frac{(\delta t)^2}{12}\frac{\mu_V}{r_{vs}^3}\dot{\bar{r}}_{vs}$$

$$+ \frac{\bar{a}}{2}(\delta t) - \frac{\dot{\bar{a}}}{12}(\delta t)^2 \qquad (65)$$

$$\bar{X} = \frac{2}{5}(\delta t)\dot{\bar{X}} + \frac{(\delta t)^2}{20}\frac{\mu_V}{r_{vs}^3}\bar{r}_{vs} + \frac{\bar{a}}{20}(\delta t)^2$$

The subscript o in the above definitions is intended to suggest that the groups of terms so designated depend only upon the conditions at the beginning of the interval. This includes terms involving the reference conic terminal conditions, since this relative trajectory is completely predetermined by the starting values. Thus, the $\bar{X}_o$ and $\dot{\bar{X}}_o$ terms are computed once only for the interval, whereas the $\bar{X}$ and $\dot{\bar{X}}$ terms are iteratively improved until there is no sensible change.

The non-point-mass terms involving $\bar{a}_o$ and $\dot{\bar{a}}_o$ properly belong in the definitions of $\bar{X}_o$ and $\dot{\bar{X}}_o$. If this acceleration contribution were dependent solely upon time (as, for example, a rocket thrust in a vacuum), then the $\bar{a}$ and $\dot{\bar{a}}$ vectors evaluated at the end of the interval also could be included in $\bar{X}_o$ and $\dot{\bar{X}}_o$. In general, however, such effects will be state-dependent (e.g., solar radiation pressure or aerodynamic forces) and hence must be iterated. Therefore, these contributions have been written in the $\bar{X}$ and $\dot{\bar{X}}$ groupings. This will result in only a slight inefficiency in unnecessarily iterating the exceptional cases of state independence. Appendix A treats methods for handling terms dependent upon $\bar{a}$ for different cases.

The final set of Eqns. (64) and (65) for propagating the spacecraft state are very simple. As derived they guarantee that the correction, given by Eqn. (47), and its next higher

derivative will be satisfied at the beginning and the end of the computing interval. This, of course, means that the original differential equation of motion, Eqn. (42) or (43), for spacecraft acceleration and its derivative for spacecraft jerk will also be satisfied at the two ends of the interval. The algebraic equations for the Virtual Mass state, Eqns. (26) and (27), will be similarly satisfied. For the sake of brevity in future references, this procedure will be called MAJ for matched acceleration and jerk.

Note that, although the combined correction solution $\bar{r}_c$ was expanded in a Taylor's series in the time increment δt to terms of degree five for position and four for velocity, the final solution for the spacecraft state is of degree three for position and two for velocity. This occurs because the inversion of Eqns. (60c, d) to solve for $\bar{\bar{\bar{\bar{r}}}}_{c_o}$ and $\bar{\bar{\bar{\bar{\bar{r}}}}}_{c_o}$ results in solutions, in Eqns. (63), involving $(\delta t)^{-2}$ and $(\delta t)^{-3}$. Thus, multipliers involving δt to higher powers are reduced, leaving no terms in δt beyond the third power. Most important from the standpoint of the practicalities of numerical computation is the fact that there are no negative powers of δt in the final forms.

The MAJ procedure can be extended to obtain higher order solutions. The system of two equations for the two unknown fourth and fifth order initial value coefficients was obtained by evaluating Eqns. (59) and (60c, d) at the end point of the interval δt, equating and solving. If the initial series expansion had been carried out to the seventh order term, these two equations (now in the four unknowns of the fourth through the seventh order coefficients) could be augmented by two more obtained by evaluating Eqns. (59) and (60c, d) at the midpoint $\left(\frac{\delta t}{2}\right)$ and equating. This would give the requisite number of four equations and would guarantee the satisfaction of all equations (acceleration and jerk) at the interval midpoint as well as the endpoints. The procedure can be extended in principle to any order desired by choosing a sufficient number of intermediate points in the computing interval. However, the algebra does get more complicated with the necessity for solving larger and larger systems of simultaneous equations for the higher order coefficients.

The MAJ procedure has been programmed only for the fifth order solution given explicitly by Eqns. (64) and (65). Detailed numerical results will be presented later. It will

simply be remarked here that this is far more accurate and faster than any of the earlier methods and the fifth order representation appears to be sufficient for anticipated requirements.

3.2 Numerical Computation Procedure

Some considerations of the numerical computation procedure for the fifth order MAJ technique are presented here. It is not the intent to document the digital computer programming details (this is done in Ref. 13), but rather to facilitate a better understanding of the method by discussing the more important numerical analysis aspects.

The iterative computation procedure is best described by means of the flow diagram shown in Figure 6. It is activated by a "CALL" from, and effects a "RETURN" to, a MAIN program which, among other things, monitors the progress along the trajectory for satisfaction of certain user-prescribed "events". If an event is not imminent, a flag named LØØP is set by the MAIN program to tell the stepwise integrator to proceed with a normal step; otherwise, the flag is set to cause a recomputation of the last step so as to end the cycle exactly at the desired event. The first action taken in Block 1, therefore, is to test the flag setting and determine whether this is to be a new step or a recalculation of the last step. If it is to be a new step, certain quantities computed at the end of the preceeding interval are indexed in Block 2 to serve as the initial values for the new step. Among these quantities are the relative state values $\bar{r}_{vs}$, $\dot{\bar{r}}_{vs}$ and μ_v which become the reference conic initial values $\bar{r}_{vr_o}$, $\dot{\bar{r}}_{vr_o}$ and μ_{v_o}. These quantities are then used in Block 3 to compute the reference conic orbital elements. Equations (3) are used with the appropriate substitutions on the right-hand sides.

The next order of business is to establish the desired computing interval size in Block 4. Based on the nature of the Virtual Mass phantom trajectory relative to the spacecraft path, it was decided in the computer mechanizations reported in Ref. 3 to try and hold essentially equal increments in true anomaly relative to the Virtual Mass. This would have the effect of automatically reducing the time interval whenever the spacecraft flies close to a celestial body (and hence close to the Virtual Mass) and increasing the time increment when displaced far from all bodies. If the desired true anomaly increment is denoted $\delta\theta$, the time increment corresponding to $\delta\theta$ can be found as (to first order)

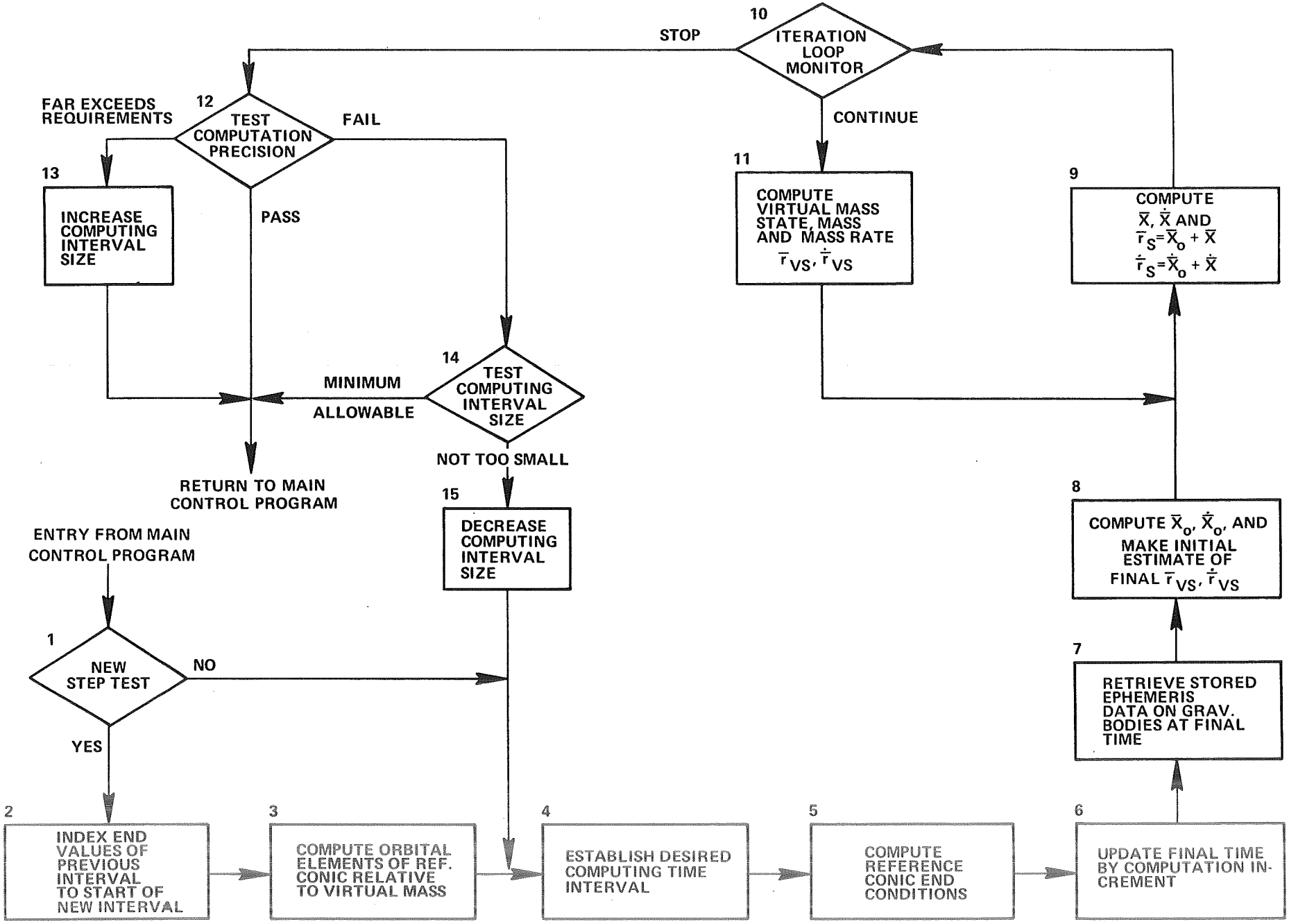

FIGURE 6 - COMPUTATION FLOW DIAGRAM FOR SIMPLE STEPWISE INTEGRATOR

$$\delta t = \frac{r_{vr_o}^2 \delta\theta}{H} \tag{66}$$

Here H is twice the instantaneous areal rate relative to the Virtual Mass and is the magnitude of the vector defined by Eqn. (3a). As noted in Ref. 3, special instances can occur where the spacecraft motion is momentarily directed precisely toward or away from the Virtual Mass. In such cases, of course, $H \equiv 0$ and Eqn. (66) is singular. In order to avoid this difficulty, H can be replaced by $r_{vr_o} V_{vr_o}$, where $V_{vr_o} = |\dot{\bar{r}}_{vr_o}|$. This is tantamount to assuming that $\dot{\bar{r}}_{vr_o}$ is orthogonal to $\bar{r}_{vr_o}$. In reality this condition is realized only for an apsidal crossing; hence, the modified form

$$\delta t = \frac{r_{vr_o} \delta\theta}{V_{vr_o}} \tag{67}$$

can be considered to give time increments corresponding to a specified increment $\delta\theta$ in "apsidal anomaly". The possibility that $V_{vr_o} \equiv 0$ is quite remote and, of course, when V_{vr_o} is small we desire large computation time intervals. The earlier programs of Ref. 3 used Eqn. (67), holding $\delta\theta$ constant at an input value. The present program, as we shall see later, does provide some intelligence for modifying $\delta\theta$ as necessary during a trajectory computation. For now, however, simply assume that Eqn. (67) is used to compute a δt corresponding to some specified $\delta\theta$. Block 4 compares this increment with the MAIN program estimate of the time to the next event and sets the desired δt to the smaller of the two.

Block 5 solves the Kepler problem for the given initial conditions on the known orbit to find the reference conic end conditions. Depending upon the setting of the flag, LØØP, the end conditions are determined either to approximate the desired time interval on the basis of the first guess, or else to iterate to precise satisfaction of the desired increment. Thus, when there is no need to iterate exactly to a prespecified

event, the computation is free-running in order to conserve computing time. The time increment calculation is accurate for the final state determined, but does not correspond exactly to the predetermined time interval except at an event.*

The conic section time increment computed in Block 5 is used in Block 6 to update the ephemeris time. In Block 7 a magnetic tape is searched to retrieve stored data giving the states of the gravitating mass points at the updated final ephemeris time. Since these data are stored at time intervals which do not in general correspond with the computed time increments, an interpolation is required to obtain data at the desired times.

Final preparations are made in Block 8 to enter the iteration loop of the computation. As a simple first estimate, the final spacecraft state relative to the Virtual Mass is set to the reference conic final state:

$$\begin{aligned} \bar{r}_{vs} &= \bar{r}_{vr} \\ \dot{\bar{r}}_{vs} &= \dot{\bar{r}}_{vr} \end{aligned} \tag{68}$$

and $\bar{X}_o$ and $\dot{\bar{X}}_o$ are computed by Eqns. (65a, b).

Block 9 begins the iterative estimation of the final spacecraft inertial state. Equations (65c, d) are used to compute $\bar{X}$ and $\dot{\bar{X}}$, and Eqns. (64) give the estimate of the final state. The iteration loop monitor in Block 10 transfers to Block 11 a fixed number of times for successive improvement of the final state estimate. This is accomplished in Block 11 by evaluating Eqns. (26) and (27) for the Virtual Mass final state corresponding to the latest update (from Block 9) of the spacecraft final state and the gravitating point mass inertial states from Block 7. The loop is closed by returning to Block 9 to update $\bar{r}_s$ and $\dot{\bar{r}}_s$. Numerical experiments have shown that convergence is very rapid to mutually compatible sets of values of spacecraft and Virtual Mass final states. Thus, the monitor in

---

*The precision of calculation of the final positions and times will be dealt with later.

Block 10 is programmed to iterate twice, then switch to the precision test in Block 12. Here the last two successive estimates of $\bar{r}_s$ are compared. If they agree to within a specified tolerance (to be discussed shortly), the cycle is considered to be completed and the program returns to the MAIN program. If $\delta\theta$, and hence δt, happens to be very small for the specified tolerance, successive position estimates will agree much better than required. In this case Block 13 will be entered, where the desired apsidal anomaly $\delta\theta$ will be increased by a factor 1.1 for subsequent steps. On the other hand, if $\delta\theta$ is too large, the precision tolerance will not be satisfied in Block 12. In this case $\delta\theta$ will be compared in Block 14 with a minimum allowable step size. If it exceeds this minimum, $\delta\theta$ is reduced in Block 15 by a factor 0.8 and the interval is recomputed, starting again at Block 4. If $\delta\theta$ has already been reduced to the minimum allowable size, the program simply returns to MAIN since it cannot meet the precision tolerance within the limits of the minimum allowable step size.

This section will be concluded with a discussion of the relationship of the precision of calculation of the reference conic to the precision of position computation. The form of Eqns. (58) shows clearly the dependence of the final solution $\bar{r}_s$ upon the reference conic $\bar{r}_{vr}$ and the combined correction $\bar{r}_c$. In the procedure just described, the reference conic contribution remains fixed, whereas the correction term is iteratively improved. Even $\bar{r}_c$ itself is composed of a fixed part $\bar{X}_o$ and a variable $\bar{X}$ which is really the iterated quantity. The computational precision test referred to in Block 12 of Fig. 6 is

$$\frac{\left|\bar{X}_n - \bar{X}_{n-1}\right|}{r_{vr}} \leq P \qquad (69)$$

where P is the required relative precision. Note that the division by r_{vr} has the effect of building a variability into the absolute precision. As the spacecraft comes very near a celestial body and hence to the Virtual Mass, a very tight tolerance is held in the position calculation. Conversely, as the spacecraft moves far away, the absolute tolerance on position is relaxed.

Since $\bar{r}_{vr}$ is computed from closed analytical forms for conic sections, one may conclude that the precision of this contribution depends solely upon the mechanics of performing these fixed operations with a given number of digits. However, the time associated with the transfer along the conic arc from $\bar{r}_{vr_o}$ to $\bar{r}_{vr}$ is computed using a recursion formula for an infinite series expansion for the time of flight (see Ref. 7). The truncation of this series is controlled by a time tolerance parameter T_{tol}. If T_{tol} is large, the series will be truncated early and the time increment δt will be in error from the correct value associated with $\bar{r}_{vr_o}$ and $\bar{r}_{vr}$. However, since time is the independent variable, the δt is taken as correct and this means that the $\bar{r}_{vr}$ must be interpreted as being incorrect for this δt.

It is clear from the foregoing discussion that there is an intimate interdependence of T_{tol} and P. If P reflects the precision desired for the calculation of $\bar{r}_s$, then T_{tol} must be compatible with it.

It is assumed that the sum of the neglected terms in the time series is less than the last one computed. The last term computed is smaller than T_{tol} since that is the truncation criterion. Thus, the absolute error in the reference conic position is bounded by

$$\varepsilon_T = T_{tol} \, |\dot{\bar{r}}_{vr}| \tag{70}$$

Converting Eqn. (69) to an expression for the bound on the absolute error of the correction contribution gives

$$|\bar{X}_n - \bar{X}_{n-1}| = |\bar{r}_{c_n} - \bar{r}_{c_{n-1}}| \equiv \varepsilon_p = Pr_{vr} \tag{71}$$

Suppose we require that the time error bound be some arbitrary factor times the position error bound:

$$\varepsilon_T = (\varepsilon_p)F \tag{72}$$

Then, substituting Eqns. (70) and (71) into Eqn. (72) and solving for T_{tol} gives

$$T_{tol} = FP \frac{r_{vr}}{|\dot{\bar{r}}_{vr}|} \tag{73}$$

From a practical standpoint Eqn. (73) is computed at the beginning of the interval, using initial rather than final values. Numerical tests have shown that optimal performance is achieved with

$$F = \frac{1}{2}$$

Since Eqn. (73) is evaluated at the beginning of the interval, a comparison of Eqns. (67) and (73) reveals that the desired time increment can be expressed simply as

$$\delta t = \beta(T_{tol}) \tag{74}$$

The factor β lumps together the constants $\delta\theta$, F and P. It is this factor that is increased in Block 13 or decreased in Block 15 according to the computational precision test results.

The only parameter which must be changed to vary the speed and accuracy of the computation is the precision control P. The smaller this number, the smaller the tolerances and the computation step sizes; the larger it is, the looser the tolerances and the faster the trajectory is computed. The next section will show numerical results demonstrating the performance capabilities.

3.3 Numerical Experiments with the Fifth Order MAJ Procedure

The best method for checking the accuracy of a numerical integration procedure is to compare it with a solution which is known in closed analytical form. The two body conic section is a known closed analytical solution, but it does not constitute a good check for the Virtual Mass technique, since in this case the Virtual Mass coincides exactly with the only gravitating mass point. Thus, the reference conic is the complete solution since the correction solution $\bar{r}_c \equiv 0$. The next best alternative

is to compute a solution to a problem which has some characteristic such as a known integral (not the complete integral). Fortunately, the restricted three-body problem provides such an alternative.

The Jacobi energy

$$C_j = \frac{\mu_1}{r_{1s}} + \frac{\mu_2}{r_{2s}} - \frac{\dot{\vec{r}}_s \cdot \dot{\vec{r}}_s}{2} - \omega(y_s \dot{x}_s - x_s \dot{y}_s) \qquad (75)$$

is a known integral of the restricted three-body problem. Here ω is the constant angular rate of the Earth-Moon line, and the spacecraft position and velocity components are given in a barycentric inertial coordinate system. The constancy of Eqn. (75) is a necessary (but not sufficient) condition which must be satisfied by any solution to the problem. Thus, the variation of C_j along such a trajectory is an index to the accuracy of the numerical procedure.

A typical free-return Earth-to-Moon transfer trajectory was used in Ref. 3 to test the accuracies of various mechanizations of the Virtual Mass technique in terms of the Jacobi energy. This same trajectory has been computed using the fifth order MAJ technique described here. The Earth-Moon system parameters and the trajectory initial conditions and gross characteristics are summarized in the following table. The inertial coordinate system is centered at the barycenter and the XY plane coincides with the Earth-Moon orbital plane. The positive Z axis is defined by the right-hand convention with respect to the Moon's orbital motion. A computer-generated plot of the trajectory is depicted in Fig. 7. The Z-component line element was swept along the trace in the XY plane to show the outbound half of the twisted three-dimensional figure-of-eight trajectory. The paths of the Moon and the Virtual Mass in the plane are also shown.

The performance of the Virtual Mass integrator in computing this trajectory in double precision is presented graphically in Figs. 8, 9, and 10. Normalized Jacobi energy variation, number of computation steps and position deviation are shown versus trajectory times for a wide range of values of the precision tolerance P. The normalization of the energy

PARAMETER OR VARIABLE		NUMERICAL VALUE
Earth-Moon distance (n. mi.)		207747.2
Angular rate of Earth-Moon line (deg/hr)		0.54901493
Ratio of Moon mass to Earth-Moon mass		0.012143289
Time (hr) before start of trajectory that Moon crossed x-axis		93.591177
Spacecraft initial position	X	- 1126.088
(n. mi.)	Y	- 5433.0951
	Z	195.9727
Spacecraft initial velocity	$\dot{X}$	18364.879
(n. mi./hr)	$\dot{Y}$	3152.5321
	$\dot{Z}$	10624.889
Initial trajectory inclination relative to Moon orbital plane		30.°
Approximate time of insertion-to-pericynthion (hr)		70.33875
Approximate pericynthion altitude (n. mi.)		210

Table 1. Typical Earth-Moon System Parameters and Trajectory Initial Conditions

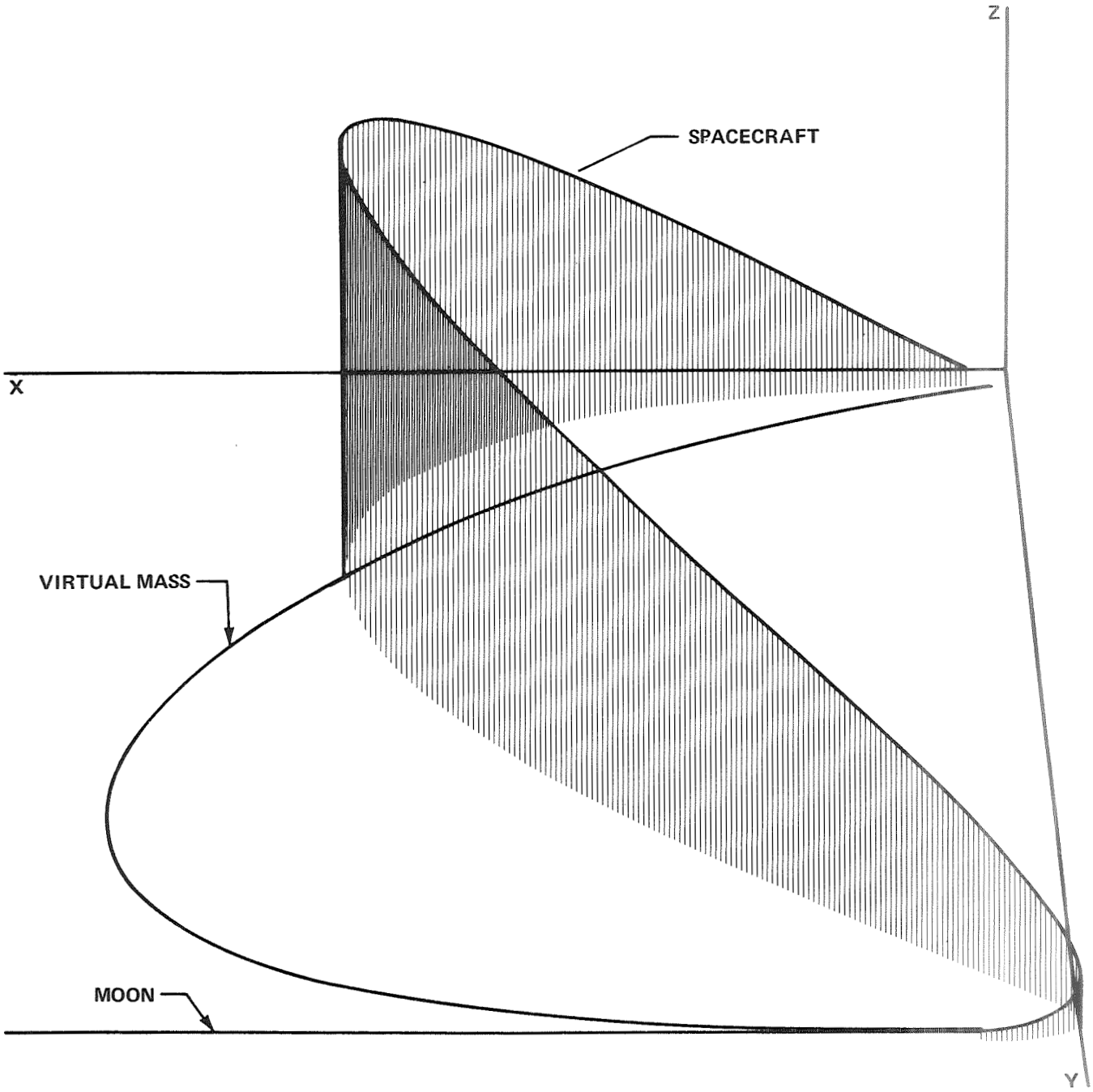

FIGURE 7 - RESTRICTED THREE BODY EARTH-TO-MOON TRAJECTORY

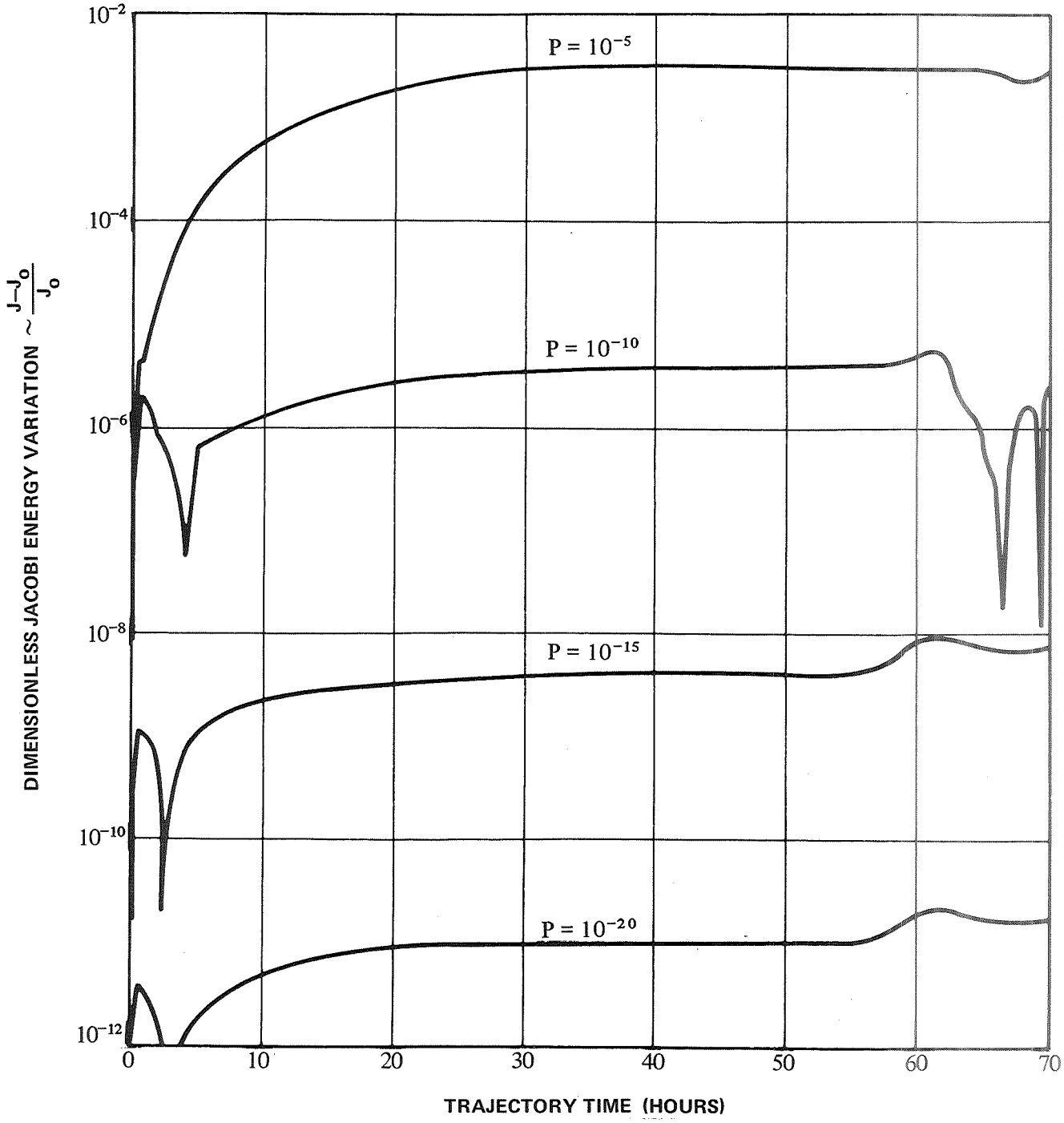

FIGURE 8 - DIMENSIONLESS JACOBI ENERGY VARIATION ALONG EXAMPLE EARTH-MOON TRAJECTORY

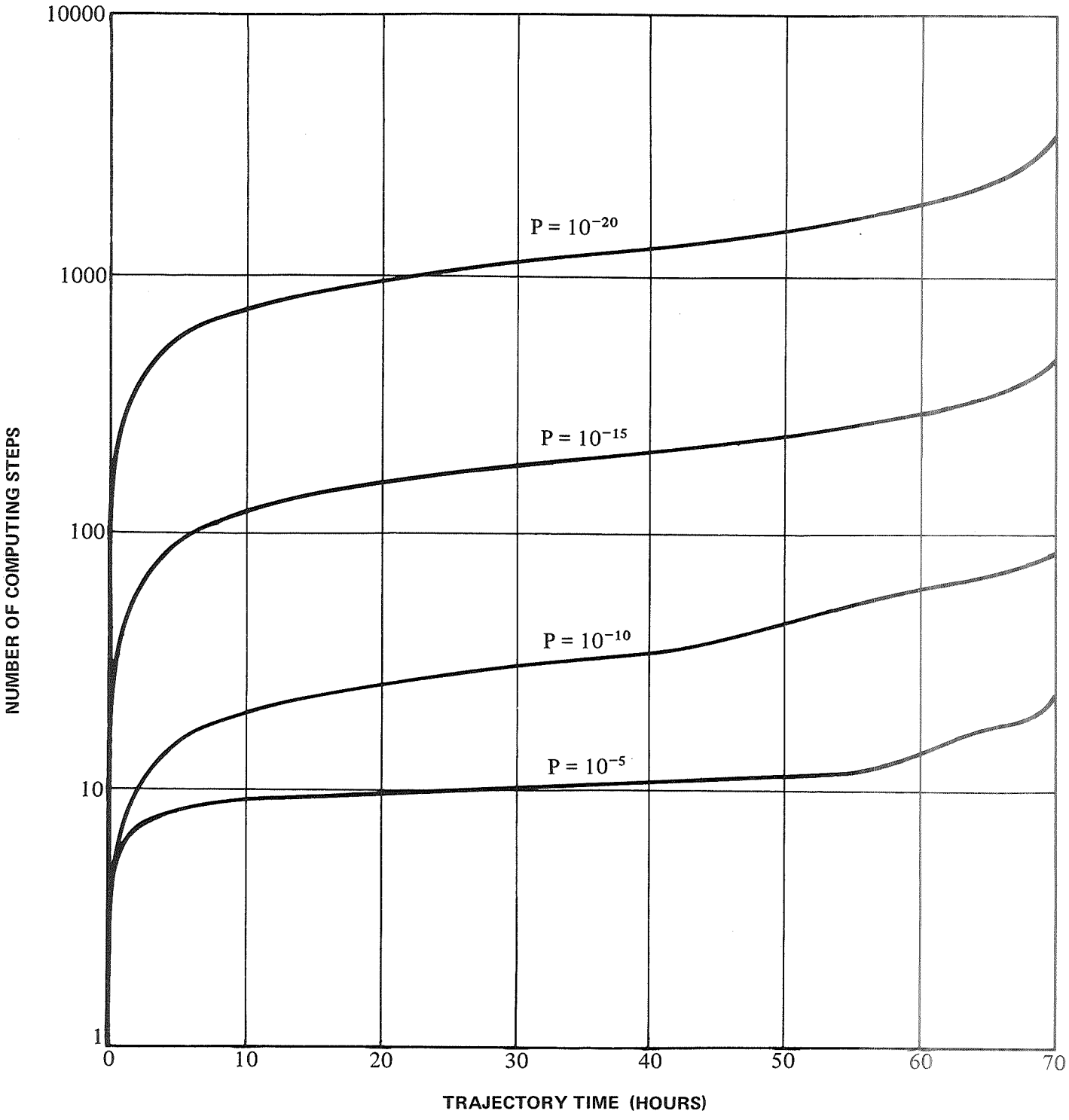

FIGURE 9 - COMPUTATION STEP COUNT VERSUS TRAJECTORY TIME FOR EXAMPLE EARTH-MOON TRAJECTORY

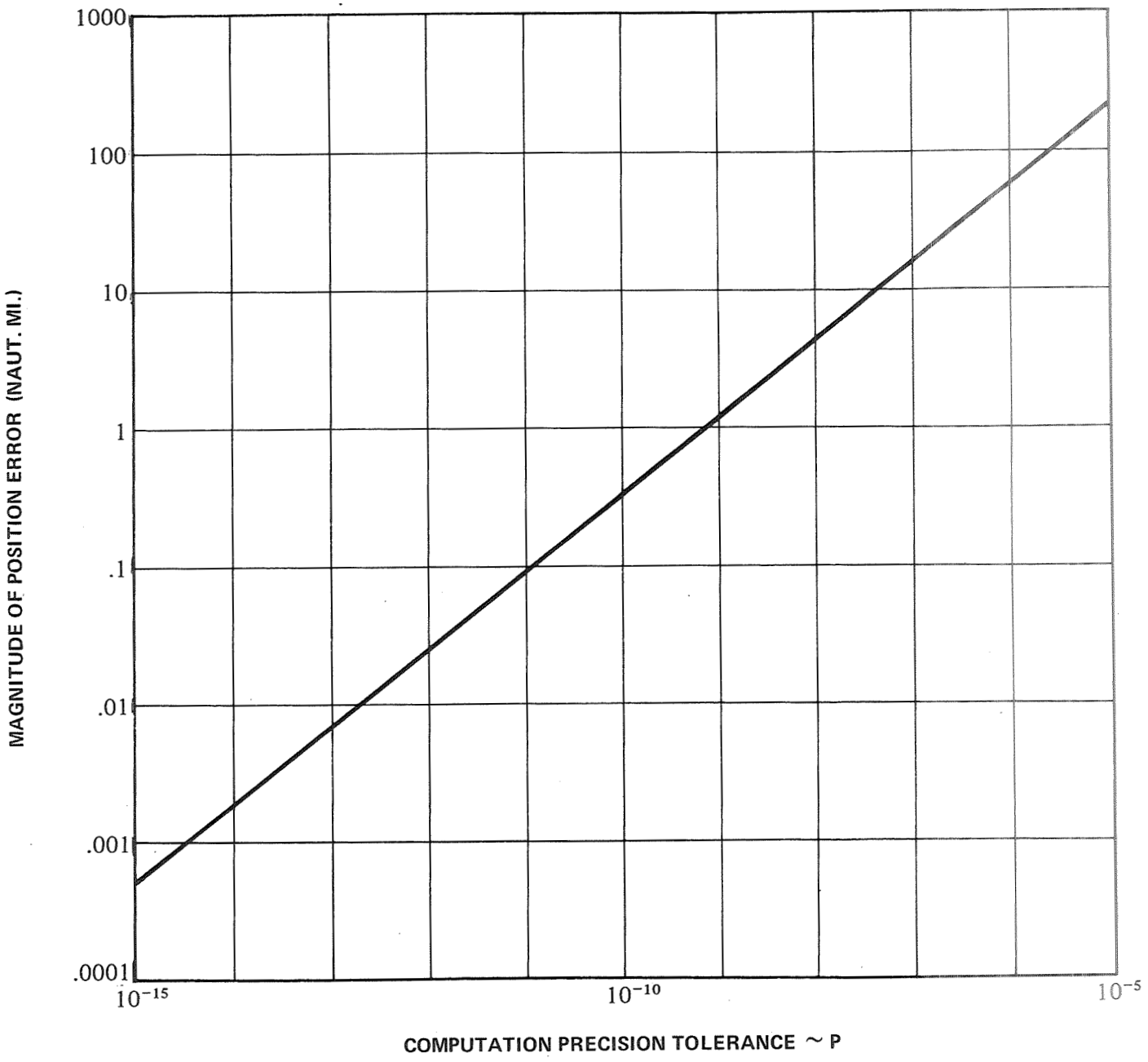

FIGURE 10 - MAGNITUDE OF POSITION DEVIATION AT FIXED FINAL TIME FOR EXAMPLE EARTH-MOON TRAJECTORY (REFERENCE IS P = 10^{-20} CASE)

variation in Fig. 8 is with respect to the initial Jacobi energy J_o:

$$\frac{J - J_o}{J_o}$$

As expected, the energy variation decreases as the precision tolerance is decreased; however, due to other factors, there appears to be little or no benefit in using a precision tolerance smaller than $P = 10^{-20}$. The price of higher accuracy is longer running time. Figure 9 shows that the high precision run was computed in a total of 3540 steps. The comparison of Figs. 8 and 9 is of particular interest. A high slope of the number of steps versus time indicates short computing time intervals and a small slope indicates longer intervals. Generally the steep slope regions of this curve correspond with the regions where the Jacobi energy variation is the greatest. Hence, one would conclude that the step size control, while perhaps not optimal, is at least behaving qualitatively in the right direction. The accuracy limitation indicated probably is inherent in the fifth order mechanization used.

At the other end of the spectrum lies the approximate solution corresponding to $P = 10^{-5}$. This trajectory was computed in only 27 steps and showed an energy variation of .0034. Figure 10 shows the positional deviation of the looser tolerance trajectories from the $P = 10^{-20}$ solution. At 70.33875 hours the $P = 10^{-5}$ trajectory deviation is 173.6 nautical miles. Note how rapidly the other trajectories converge to the accurate solution with increasingly tight tolerance specification. Clearly, for all practical purposes, lunar trajectories can be computed with precision tolerances of $P = 10^{-15}$ or looser. In fact, single precision calculation would be adequate for such trajectories. The purpose here, however, is to develop a higher precision program suitable for efficiently computing interplanetary spacecraft trajectories or planetary ephemerides. Numerical results for this type of application will be discussed next.

The 221 day Earth-to-Mars trajectory shown in Fig. 4 was computed by the Virtual Mass technique and compared with the same trajectory computed using the JPL Double Precision Trajectory (DPTRAJ) Program (Ref. 6). The flags were set

appropriately in the various options of DPTRAJ so that there was no planetary oblateness, no solar radiation pressure and no relativistic effect. Both programs used the same planetary ephemeris, DE19, the same planetary masses, and the same scaling of the solar system in kilometers. Thus, every effort was made to ensure that both programs were solving identical mathematical problems on the same computer (UNIVAC 1108 under an Exec 8 system). Only the methods of numerical integration differed.

Figure 11 summarizes the results of a series of runs with the Virtual Mass program. The magnitude of the position difference from the JPL-computed value at a fixed final time (corresponding to closest approach to Mars) is plotted versus the number of computing steps. Points along this curve are parameterized by different values of the precision tolerance P, as shown for a few cases. The agreement with DPTRAJ is quite good ($\approx$ 609 m) for the high accuracy case with $P = 10^{-18}$. This computation was performed with 979 steps and required approximately 35 seconds of central processor unit (CPU) time. The looser-tolerance case for $P = 10^{-9}$ looks especially interesting. Note that the trajectory was computed in only 70 steps and shows an error from the JPL position of slightly more than 2600 km. Thus the Virtual Mass procedure is capable of computing a good approximation very rapidly and can then be tightened down to produce a high precision solution in a still respectable time.

4.0 ASPHERICAL GRAVITATIONAL POTENTIALS

The question of the representation of non-spherical gravitational potentials of individual celestial bodies will now be considered. Two approaches are possible within the framework of the MAJ implementation described in the preceeding chapter.

(1) Expansion of the potential in spherical harmonics.

(2) Representation of the gravitational field as the superpositioning of the fields of a collection of many discreet mass points.

4.1 Spherical Harmonics

The gravitational potential function of a celestial body has traditionally been represented by a series expansion in spherical harmonics. A general form of such expansions can be written as (Ref. 8)

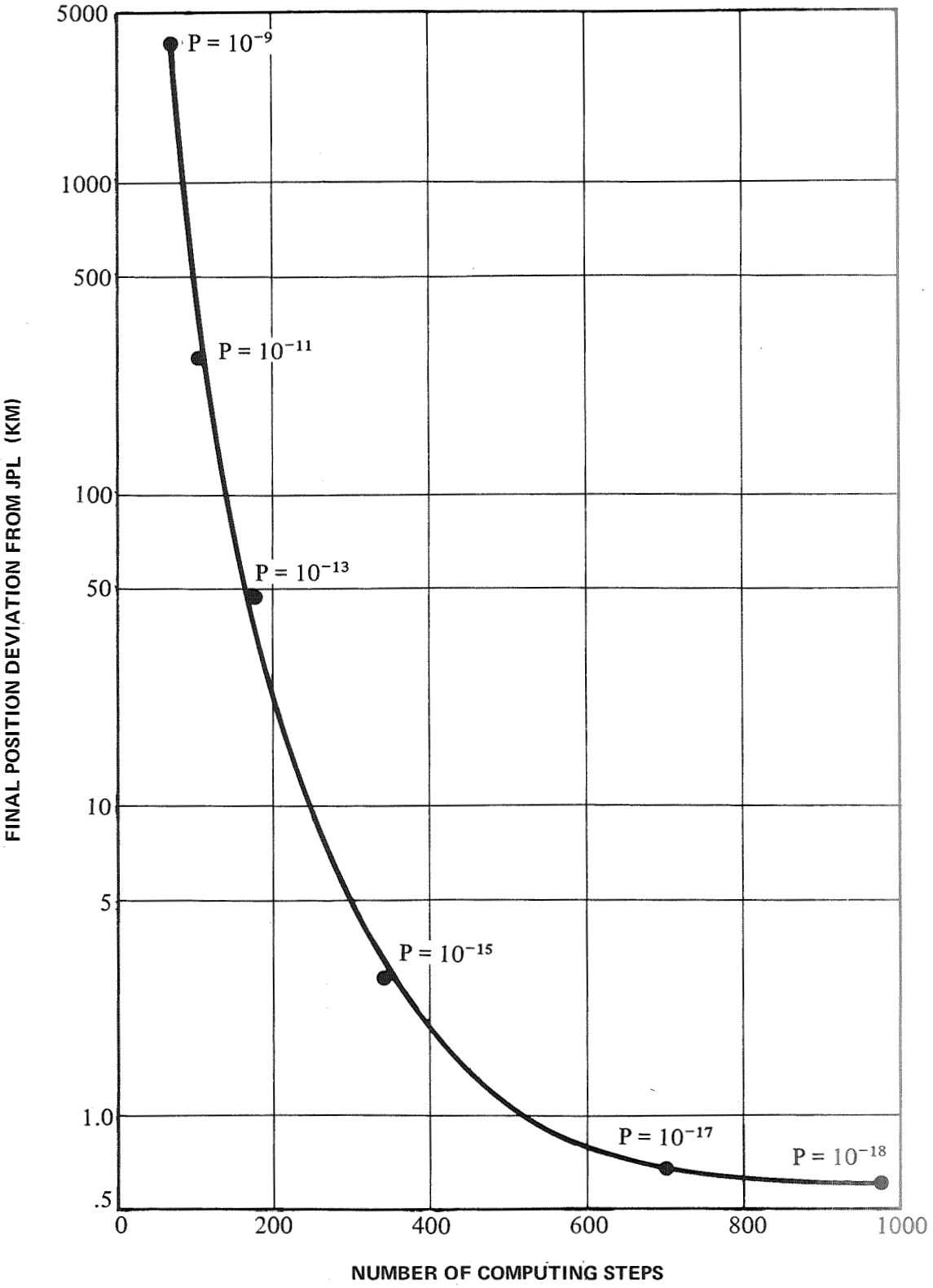

FIGURE 11 - DEVIATION OF FINAL POSITION FROM JPL-COMPUTED VALUE, FOR A 221 DAY EARTH-MARS TRAJECTORY, AS A FUNCTION OF NUMBER OF COMPUTATION STEPS

$$U = \frac{\mu}{r_s}\left[1 + \sum_{n=1}^{\infty}\sum_{m=0}^{n}\left(\frac{r_e}{r_s}\right)^n P_n^m(\sin\phi)\left(C_{nm}\cos m\lambda + S_{nm}\sin m\lambda\right)\right] \quad (76)$$

where

r_e = mean equatorial radius of planet

ϕ = satellite latitude (positive north)

λ = satellite longitude (positive east)

C_{nm}, S_{nm} = numerical coefficients ($C_{no} = -J_n = C_n$ and $S_{no} = 0$)

$P_n^m(x)$ = associated Legendre polynomial

$$= (1-x^2)^{\frac{1}{2}m}\frac{d^m P_n(x)}{dx^m}$$

$P_n(x)$ = Legendre polynomial

$$= \frac{1\cdot 3\cdot 5\cdot\cdots\cdot(2n-1)}{n!}\left\{(x)^n - \frac{n(n-1)}{2(2n-1)}(x)^{n-2}\right.$$

$$\left. + \frac{n(n-1)(n-2)(n-3)}{2\cdot 4\cdot(2n-1)(2n-3)}(x)^{n-4} - \cdots\right\}$$

The gradient of this potential is the gravitational acceleration of the spacecraft by the nearby celestial body:

$$\ddot{\bar{r}}_s = \text{grad } U = -\frac{\mu \bar{r}_s}{r_s^3} + \Delta\bar{a} \quad (77)$$

The first term on the right obviously comes from the first term on the right side of Eqn. (76). The remaining terms $\Delta\bar{a}$ derive from the double summation of terms in Eqn. (76) and will not be written out since they are algebraically quite complex. Note that the first term is the familiar single mass point contribution and represents the field attraction which would result if all the planetary mass were concentrated at the center. It can be included in the Virtual Mass computation in the usual fashion. The remaining $\Delta\bar{a}$ terms, however, define the departure from sphericity and must be included in the catchall term $\bar{a}$.

Recalling (see Eqns. (65)) that the MAJ technique requires a knowledge of $\dot{\bar{a}}$ as well as $\bar{a}$, evaluated at the computing interval end points, we see that two courses of action are possible. The first would compute $\Delta\dot{\bar{a}}$ explicitly as

$$\Delta\dot{\bar{a}} = (\dot{\bar{r}}_s \cdot \nabla)\Delta\bar{a} + \frac{\partial(\Delta\bar{a})}{\partial t} \tag{78}$$

Here the scalar operator is defined as

$$(\dot{\bar{r}}_s \cdot \nabla) \triangleq \dot{x}\frac{\partial}{\partial x} + \dot{y}\frac{\partial}{\partial y} + \dot{z}\frac{\partial}{\partial z}$$

in rectangular coordinates. In Eqn. (78) the total time rate of change of $\Delta\bar{a}$ is implied as seen by the inertially moving spacecraft. Thus the first term represents the change produced by the relative translation of the spacecraft through a rotationally static field. The second term takes account of the change seen by a spacecraft with no relative motion in a field moving rotationally with the planet. The algebraic expression for $\Delta\dot{\bar{a}}$ will be even more complex than that for $\Delta\bar{a}$, hence it also will not be written out explicitly.

The second alternative for determining $\Delta\dot{\bar{a}}$ involves a numerical procedure which requires the explicit form for $\Delta\bar{a}$ only. This is described in detail in the Appendix for the term $\bar{a}$ in general.

In principle, an arbitrary potential field can be represented rigorously by the infinite series of spherical harmonic terms. In actual practice, of course, the series must be truncated to a finite number of terms. This truncation produces only small errors in the representation of gravitational anomalies which are periodic in character. The reason for this, of course, is the periodic nature of the trigonometric terms in the series. This very characteristic of the series, however, makes it difficult to account accurately for randomly distributed local anomalies. There is evidence of the existence of discontinuous concentrations of matter within small volumes just under the surface of the Moon (Ref. 9). In fact, one would expect such mass discontinuities to exist in virtually all planetary bodies due to meteoritic impacts and/or lava or heavy ore deposits in the crusts.

Some alleviation of this practical difficulty is afforded by selective processing of short and long data arcs for satellites with a variety of orbital characteristics. However, the disagreement (by orders of magnitude) between different investigators in the higher order terms of the Earth's potential indicates the need for improvement in the theoretical approach to the problem.

4.2 Discreet Mass Points

The idea of representing a large celestial body by a collection of mass points which are fixed relative to each other is not new. In fact, the concept of microscopic subdivision of the matter in a body down to the molecular level is philosophically rather old. Essentially such a fine subdivision amounts to a representation by infinitely many particles; hence, the mathematical invention of the continuum was introduced. This led rather directly to the early adoption of the spherical harmonic approach.

Here we return to this discreet mass point representation and ask whether one can (by analogy with the truncation of the spherical harmonic series) model the potential by means of a comparatively small finite number of mass points. This subject has received surprisingly little attention from a theoretical point of view. The reader is referred to Ref. 10 for a treatment of some of the basic considerations.

There is a fundamental difference between the spherical harmonic and point mass approaches. In general, a finite

number of mass points requires an infinite harmonic series for equivalent representation and vice versa. In Ref. 10, for example, the oblate potential of the 3 mass point configuration of Fig. 12 was compared with that for a homogeneous spheroid as given in terms of an infinite spherical harmonic expansion. The comparison was done on the basis of the value of the integral, over all space outside the body, of the square of the difference between the two potentials. The condition for the minimum of this integral gives a functional relationship of m_n and h, where the total mass $m = m_p + 2m_n$ is held constant. Although the simple 3 mass point configuration cannot be made to match the given infinite series potential exactly, it can be shown that the minimized integral function vanishes as $h \to 0$, $m_n \to -\infty$ and $m_p \to +\infty$ for the simple J_2 truncated model of an oblate field. To gain some feeling for the numbers which may be used in a practical case, the minimizing criterion gives (for h = 10 miles, r_e = 4000 miles, J_2 = .0011) $m_n = -88m_e$ and $m_p = 177m_e$, where m_e is the total mass of the Earth.

This indicates that the gross departures from sphericity (e.g., polar flattening or triaxiality) are representable by large positive and negative mass points (multipoles) located close to the center of the celestial body. The comparatively small and highly localized crustal effects would then be represented by small mass points located a small distance beneath the planetary surface. Large or small, positive or negative, close-in or far-out, the important consideration is that all of these mass points can be included in the Virtual Mass computation procedure in exactly the same way as all other mass points. Therefore, the point mass approach does not suffer from increasingly complex algebra with addition of more and more terms as does the spherical harmonic approach. It simply means many more masses to be processed in the same way. This has an obvious advantage in electronic digital computation. Even this inconvenience can

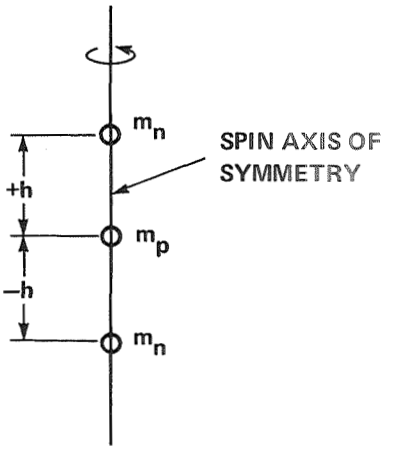

FIGURE 12 - GEOMETRY OF 3 MASS POINT OBLATE BODY

be minimized, analogous to the practice of turning off spherical harmonic expansions when sufficiently far displaced from irregular celestial bodies. Equation (38) gives the criterion by which one can precompute the distance from the center of mass of a celestial body beyond which the computational precision allows the aspherical mass points to be coalesced into a single point at the center of mass. The method of applying the two-mass-point criterion to a large assemblage of points for a given body will be shown in an illustrative example.

First suppose we choose a desired precision of

$$\frac{r_{cv}}{r_{cs}} = 3 \times 10^{-9} \ .$$

For spacecraft distances of 1 AU = 93×10^6 miles and 1 lunar distance = 240,000 miles, this precision corresponds to distances of .279 miles and 3.8 ft. respectively. Two different kinds of mass point pairs out of an aggregate used to represent the Earth are considered.

One kind consists of a large central mass point m_e, which is essentially the total Earth mass, located very close to the center of mass, and a small peripheral mass point $6 \times 10^{-6}\ m_e$, representing a heavy concentration near the surface. Take the separation distance as the Earth's radius $r_{12} = r_e = 4000$ miles. Substituting these data into the first form of Eqn. (38) gives:

$$r_{cs} = \sqrt{\frac{18 \times 10^{-6}}{3 \times 10^{-9}}}\ (4000) = 310{,}000 \text{ miles}$$

Thus, a mass concentration near the surface of 6×10^{-6} of the total Earth mass can influence position computations by about 4 ft. at a distance of 310,000 miles.

The second kind of mass point pair consists of the two negative masses of the three point configuration in Fig. 12. Using the h = 10 mile value assumed in the earlier

example, and using the second computational form of Eqn. (38):

$$r_{cs} = \sqrt{\frac{3(100)}{3 \times 10^{-9}}} = 316{,}000 \text{ miles} .$$

The data were deliberately chosen so that these two cutoff distances are nearly the same. It illustrates the point that a surface concentration must be unrealistically large to be as influential as the gross oblateness effect at large distances.

5. SUMMARY AND CONCLUSIONS

The fifth order matched acceleration and jerk implementation of the Virtual Mass concept is a simple, self-starting, fast and highly accurate method of numerically integrating a spacecraft trajectory. This procedure represents an improvement of several orders of magnitude over previous methods using the Virtual Mass. It appears to be at least competitive with, and possibly superior to, more conventional n-body integration methods.

This procedure can easily handle aspherical gravitational effects of individual celestial bodies and non-gravitational accelerations of the spacecraft such as rocket thrust, solar radiation pressure and aerodynamic forces.

Further improvements in this implementation of the Virtual Mass technique should include the development of compatible orbit determination programs. This would include development of equations for the state transition matrix using the Virtual Mass formulation. The intent would be to provide the capability to determine (a) spacecraft orbits from tracking data, (b) solar system ephemerides from astronomical observations, and (c) aspherical gravitational potentials (preferably in the form of mass points) of individual planetary bodies from satellite tracking data.

Other desirable objectives would be to determine a method of including relativistic effects and to extend the procedure described here to permit a simultaneous integration of all N bodies considered to obtain their respective orbits for a set of prescribed initial conditions.

D H Novak

2011-DHN-vh

D. H. Novak

Attachment
Appendix

REFERENCES

1. Battin, R. H., Astronautical Guidance, McGraw-Hill, New York, 1964.

2. Gartmann, H., Raumfahrtforschung, R. Oldenbourg, Munchen, 1952.

3. Novak, D. H., "Virtual Mass Technique for Computing Space Trajectories," ER 14045, Martin Co., Baltimore, Maryland, January 1966.

4. Sperling, H. J., "An Improved Description of the Varicentric Method of Space Flight Computation," Report MTP-AERO-61-1, Marshall Space Flight Center, Huntsville, Alabama, January 18, 1961.

5. Novak, D. H., "Two-Body Midcourse Navigation and Guidance for Lunar Missions," AIAA Paper 64-649, Astrodynamics Guidance and Control Conference, Los Angeles, California, 1964.

6. Devine, C. J., "JPL Development Ephemeris Number 19," Technical Report 32-1181, Jet Propulsion Laboratory, Pasadena, California, November 15, 1967.

7. Novak, D. H., "Computationally Convenient Forms for Conic Section Equations," Memorandum for File B71 01045, Bellcomm, Inc., Washington, D. C., January 8, 1971.

8. Byerly, W. E., An Elementary Treatise on Fourier's Series and Spherical, Cylindrical and Ellipsoidal Harmonics with Applications to Problems in Mathematical Physics, Dover Publications, New York, 1959.

9. Muller, P. M., and Sjogren, W. L., "Mascons: Lunar Mass Concentrations," Science, Vol. 161, No. 3842, August 16, 1968.

10. McLaughlin, W. I., "Representation of a Gravitational Potential with Fixed Mass Points," Memorandum for File B68 12109, Bellcomm, Inc., Washington, D. C., December 23, 1968.

11. Jessup, R. F., "The Univac 1108 Virtual Mass Trajectory Simulation Program," Memorandum for File B71 03073, Bellcomm, Inc., Washington, D. C., March 30, 1971.

APPENDIX

The discussion in Section 3.1 assumed that the acceleration term $\bar{a}$ (including everything but the point mass gravitational terms) and its derivative $\dot{\bar{a}}$ were known. In some instances contributions to $\bar{a}$ such as solar radiation pressure terms or spherical harmonic gravitational anomalies (see Chapter 4) may be given in explicit analytical forms. If these forms are not too complicated, the derivative $\dot{\bar{a}}$ can be written out and both expressions evaluated from the analytic forms. In many cases, however, the phenomena may be so involved as to defy reasonable analytical representation. A good example is the hypersonic aerodynamic force on a complex-shaped vehicle. The usual engineering practice is to tabulate the force (acceleration) as an empirically or experimentally determined function of its significant variables. It may also happen that the analytic form for $\bar{a}$, even though known, may be so complicated that it is impractical to differentiate in closed analytic form.

Consequently, a method may be needed to estimate $\dot{\bar{a}}$ from computed or tabulated values of $\bar{a}$. The simplest and most straightforward approach is to represent $\bar{a}$ in a Taylor's series expansion, determine the coefficients from an appropriate number of evaluations of $\bar{a}$ within the computing interval and then compute $\dot{\bar{a}}$ from the derived series. Details are presented for two cases: (1) where $\bar{a}$ is independent of the spacecraft state, and (2) where $\bar{a}$ is dependent on the state.

In terms of a truncated Taylor's series, $\bar{a}$ and its first time derivative are

$$\begin{cases} \bar{a} = \bar{c}_o + \bar{c}_1(\delta t) + \dfrac{\bar{c}_2}{2}(\delta t)^2 + \ldots. + \dfrac{\bar{c}_n}{n!}(\delta t)^n \\ \dot{\bar{a}} = \bar{c}_1 + \bar{c}_2(\delta t) + \dfrac{\bar{c}_3}{2}(\delta t)^2 + \ldots.. + \dfrac{\bar{c}_n}{(n-1)!}(\delta t)^{n-1} \end{cases} \tag{A-1}$$

Since $\bar{a}_o = \bar{c}_o$ is known, there are n coefficients $\bar{c}_1, \ldots, \bar{c}_n$ to be determined. If $\bar{a}$ is evaluated at n points (not including the beginning point $\bar{a}_o$ of the interval), a sufficient number of equations can be obtained to invert for the unknown coefficients. Denote a sequence of n non-zero different proper fractions ending with unity by $f_j (j=1,\ldots,n)$, $f_n = 1$. Use these to designate a sequence of time points across the computing interval as $\delta t_j = f_j \, \delta t$. The corresponding values of $\bar{a}$ are denoted $\bar{a}_j$. In this notation, the system of equations representing n different evaluations of Eqn. (A-1a) is written as

$$\begin{bmatrix} \bar{a}_1 \\ \bar{a}_2 \\ \vdots \\ \bar{a}_n \end{bmatrix} = \begin{bmatrix} \bar{a}_o \\ \bar{a}_o \\ \vdots \\ \bar{a}_o \end{bmatrix} + (\delta t) F \begin{bmatrix} \bar{c}_1 & & & \\ & \bar{c}_2 (\delta t) & & \\ & & \ddots & \\ & & & \dfrac{\bar{c}_n}{(n-1)!} (\delta t)^{n-1} \end{bmatrix} \tag{A-2}$$

where the matrix is

$$F = \begin{bmatrix} f_1 & \dfrac{f_1^2}{2} & \dfrac{f_1^3}{3} & \cdots & \dfrac{f_1^n}{n} \\ f_2 & \dfrac{f_2^2}{2} & \dfrac{f_2^3}{3} & \cdots & \dfrac{f_2^n}{n} \\ \vdots & \vdots & \vdots & \cdots & \vdots \\ 1 & \dfrac{1}{2} & \dfrac{1}{3} & \cdots & \dfrac{1}{n} \end{bmatrix} \tag{A-3}$$

The inversion to solve for the coefficients is written formally as:

$$\begin{bmatrix} \bar{c}_1 \\ \bar{c}_2(\delta t) \\ \vdots \\ \frac{\bar{c}_n}{(n-1)!}(\delta t)^{n-1} \end{bmatrix} = (\delta t)^{-1} F^{-1} \begin{bmatrix} \bar{a}_1 - \bar{a}_o \\ \bar{a}_2 - \bar{a}_o \\ \vdots \\ \bar{a}_n - \bar{a}_o \end{bmatrix} \qquad \text{(A-4)}$$

It is at this point that a distinction is made between the state-dependent and state-independent cases.

If $\bar{a}$ depends only upon time and is independent of the spacecraft state, the fractional subdivisions f_j of the interval can be predetermined at convenient fixed values. This means that the matrix F^{-1} could be pre-computed and pre-programmed to solve Eqn. (A-4) directly for the coefficients $\bar{c}_j$ for appropriate values of $\bar{a}_o, \ldots, \bar{a}_n$. For example, if n is chosen as 3 and $f_1 = \frac{1}{3}$, $f_2 = \frac{2}{3}$, $f_3 = 1$,

$$F = \begin{bmatrix} \frac{1}{3} & \frac{1}{18} & \frac{1}{81} \\ \frac{2}{3} & \frac{2}{9} & \frac{8}{81} \\ 1 & \frac{1}{2} & \frac{1}{3} \end{bmatrix}$$

and

$$F^{-1} = \begin{bmatrix} 9 & -\frac{9}{2} & 1 \\ -45 & 36 & -9 \\ \frac{81}{2} & -\frac{81}{2} & \frac{27}{2} \end{bmatrix}$$

These cases of state-independence permit the complete determination of $\bar{a}$ and $\dot{\bar{a}}$ at the beginning of the computing interval. The terms involving $\bar{a}$ and $\dot{\bar{a}}$ can be eliminated from Eqns. (65c, d) for $\bar{X}$ and $\dot{\bar{X}}$ and can be included in Eqns. (65a, b) for $\bar{X}_o$ and $\dot{\bar{X}}_o$.

When $\bar{a}$ does depend upon the spacecraft state, the determination of the coefficients $\bar{c}_j$ becomes considerably more complicated. Evaluation of the spacecraft state at points interior to the computing interval has not been provided in the fifth order MAJ procedure described in Chapter 3. It could be done, however, with some obvious modifications of the flow diagram described there and shown in Fig. 6. These changes would also be necessary (regardless of how $\bar{a}$ is given) if the MAJ procedure were to be extended beyond the fifth order.

Basically, a capability must be provided for multiple evaluations of Blocks 5 through 9 and Block 11. The desired computing interval, determined in Block 4, must be subdivided into the specified number of parts. This is most easily done by initially setting $f_j = \frac{j}{n}$. The desired δt_j determined in this manner would be matched only approximately in the free-running mode described in Section 3.2 for the reference conic evaluations in Block 5. The only exception would be that $f_n = 1$, or δt, would be iterated exactly at an event. The time increments δt_j actually achieved in Block 5 would then be used in Block 6 to obtain the required sequence of n updated ephemeris times. The ephemeris tape search and data interpolation would be conducted in Block 7 as necessary to obtain the states of the gravitating mass points at the n time points.

The preparations made in Block 8 to enter the iteration cycle must be expanded to provide for multiple evaluation (once at each of the n points) of Eqns. (68) and (65a, b). Note that in these equations the quantities $\bar{r}_{vs}$, $\dot{\bar{r}}_{vs}$, $\bar{r}_{vr}$, $\dot{\bar{r}}_{vr}$, $\bar{X}_o$, $\dot{\bar{X}}_o$, and δt would all be further subscripted with the letter j. Note also that the terms involving $\dot{\bar{a}}_o$ would be eliminated from Eqns. (65a, b) for $\bar{X}_{o_j}$ and $\dot{\bar{X}}_{o_j}$ and moved to Eqns. (65c, d) for $\bar{X}_j$ and $\dot{\bar{X}}_j$. This is because $\dot{\bar{a}}_o = \bar{c}_1$ is not fixed a priori but must be iterated.

Two additional functions must be performed in Block 8. The first is the estimation of values of $\bar{a}_j$. The value of $\bar{a}$ at the end of the preceding interval is indexed to be the initial value for the new:

$$\bar{c}_o = \bar{a}$$

The remaining coefficients $\bar{c}_1, \ldots, \bar{c}_n$ would be left at their previous values as a first guess for the iteration procedure. For the starting step of a trajectory, these coefficients would be initialized to zero. Finally, Eqn. (A-1a) can be used repeatedly to compute the first estimates of a_j.

The second additional function is the computation of the matrix F^{-1}. The $f_j \neq \frac{j}{n}$ since the free-running mode in Block 5 does not iterate the δt_j accurately to the desired values. Therefore Block 8 would compute the actual fractions as

$$f_j = \frac{\delta t_j}{\delta t}$$

This would permit the evaluation of Eqn. (A-3) for F. Finally a standard inversion procedure would yield F^{-1}.

Equations (64) and (65c, d) are computed in Block 9 for each of the n time points to obtain the corresponding estimates of the spacecraft state. Before this can be done, however, Eqns. (A-1b) must be computed to evaluate $\dot{\bar{a}}_j$. The initial value $\dot{\bar{a}}_o$ is simply $\bar{c}_1$.

Block 11 is where the equation or tabulated values for $\bar{a}$ are required in order to determine the $\bar{a}_j$ corresponding to the latest spacecraft state estimates $\bar{r}_{s_j}$ and $\dot{\bar{r}}_{s_j}$. Equations (A-4) can then be used to update the coefficients $\bar{c}_j$. These data, together with the Virtual Mass parameters, permit the iteration loop to be closed by returning to Block 9. The iteration logic and computational precision control are the same as previously described in Section 3.2.

Clearly the evaluation of the spacecraft state at interior points greatly increases the amount of computation per interval. The allowable step size for a prescribed accuracy, therefore, would have to be more than proportionately larger for this approach to pay off. One should also bear in mind that when the $\bar{a}$ values are experimentally determined, the accuracy is characteristically not very high. Accordingly, there is some justification for using an integration procedure whose accuracy is commensurate with the data. This may suggest using n = 1 -- that is, reducing Eqn. (A-1) to

$$\bar{a} = \bar{c}_o + \bar{c}_1(\delta t)$$

$$\dot{\bar{a}} = \bar{c}_1$$

and determining $\bar{c}_1$ from the end-values only. This, of course, reduces to the simple modified Euler integrator for the non-point-mass acceleration terms $\bar{a}$, but this may be entirely appropriate to the situation.